19 SEP 1997

REPORT DOCUMENTATION PAGE

Form Approved
OMB No. 0704-0188

1. AGENCY USE ONLY (Leave blank)	2. REPORT DATE	3. REPORT TYPE AND DATES COVERED
	8/31/97	Final Report, 9/1/94 - 8/31/97

4. TITLE AND SUBTITLE
(U) Ignition and Flame Stabilization in High Speed Flows

5. FUNDING NUMBERS
PE - 61103D
PR - 3484
SA - WS
G - F49620-94-1-0391

6. AUTHOR(S)
Chung K. Law

7. PERFORMING ORGANIZATION NAME(S) AND ADDRESS(ES)
Princeton University
Department of Mechanical & Aerospace Engineering
Princeton, NJ 08544

8. PERFORMING ORGANIZATION REPORT NUMBER
AFOSR-TR
97-0404

9. SPONSORING/MONITORING AGENCY NAME(S) AND ADDRESS(ES)
AFOSR/NA
110 Duncan Avenue, Suite B115
Bolling AFB DC 20332-0001

10. SPONSORING/MONITORING AGENCY REPORT NUMBER

11. SUPPLEMENTARY NOTES

12a. DISTRIBUTION/AVAILABILITY STATEMENT
Approved for public release; distribution is unlimited

12b. DISTRIBUTION CODE

13. ABSTRACT (Maximum 200 words)

Reduced mechanisms for ignition of hydrogen by heated air were deduced for the high-temperature/low-pressure and the low-temperature/high-pressure regimes. The reduced mechanisms were subsequently applied to the physical situations of the supersonic mixing layer and the counterflow through numerical simulation and activation energy asymptotics. Various ignition criteria were derived, and the issues of thermal versus radical induced ignition, external versus internal heating in inducing ignition, and quasi-steady versus transient ignition, were explored.

14. SUBJECT TERMS
Supersonic combustion, ignition, flame stabilization, hydrogen/air ignition, reduced mechanisms

15. NUMBER OF PAGES
44

16. PRICE CODE

17. SECURITY CLASSIFICATION OF REPORT	18. SECURITY CLASSIFICATION OF THIS PAGE	19. SECURITY CLASSIFICATION OF ABSTRACT	20. LIMITATION OF ABSTRACT
Unclassified	Unclassified	Unclassified	UL

AUGMENTATION AWARDS FOR SCIENCE & ENGINEERING RESEARCH TRAINING (AASERT) REPORTING FORM

The Department of Defense (DoD) requires certain information to evaluate the effectiveness of the AASERT Program. By accepting this Grant which bestows the AASERT funds, the Grantee agrees to provide 1) a brief (not to exceed one page) narrative technical report of the research training activities of the AASERT-funded student(s) and 2) the information requested below. This information should be provided to the Government's technical point of contact by each annual anniversary of the AASERT award date.

1. Grantee identification data: (R&T and Grant numbers found on Page 1 of Grant)

a. Princeton University
University Name

b. F49620-94-1-0391
Grant Number

c. 3484/WS
R&T Number

d. C.K. Law
P.I. Name

e. From: 7/15/96 To: 7/14/97
AASERT Reporting Period

NOTE: Grant to which AASERT award is attached is referred to hereafter as "Parent Agreement".

2. Total funding of the Parent Agreement and the number of full-time equivalent graduate students (FTEGS) supported by the Parent Agreement during the 12-month period prior to the AASERT award date.

a. Funding: $ 0

b. Number FTEGS: 0

3. Total funding of the Parent Agreement and the number of FTEGS supported by the Parent Agreement during the current 12-month reporting period.

a. Funding: $ 125,000

b. Number FTEGS: 2

4. Total AASERT funding and the number of FTEGS and undergraduate students (UGS) supported by AASERT funds during the current 12-month reporting period.

a. Funding: $ 53,000

b. Number FTEGS: 1

c. Number UGS: 0

VERIFICATION STATEMENT: I hereby verify that all students supported by the AASERT award are U.S. citizens.

Chung K. Law
Principal Investigator Chung K. Law

9/17/97
Date

Final Report

The objective of the present program, as stated in the proposal, was to theoretically study the ignition and flame stabilization of hydrogen in air in high-speed flows. Emphasis was on computational study of the structure of the chemically reacting high-speed flows with realistic chemistry, derivation of reduced mechanisms of the reaction system, and asymptotic analysis of the reaction zone structure and the flame response. This objective was satisfactorily accomplished, as summarized in the following and reported in detail in the four archival publications that have so far resulted from the present program.

A numerical study of the ignition in the supersonic mixing layer with detailed transport and chemical reaction mechanisms was first conducted. The emphasis of the study was on identifying the controlling chemical mechanism in effecting ignition, on the roles of thermal versus kinetic-induced ignition in which heat release and hence nonlinear thermal feedback are not needed in initiating system runaway, and on the consequences of imposing the conventional constant property assumptions in the previous analytical study. Results show that the state of the hydrogen/oxygen second explosion limit has the dominant influence in the system response in that, for all practical purposes ignition is not possible when the air stream temperature is lower than the crossover temperature, even allowing for viscous heating. On the other hand, when the air stream temperature is higher than the crossover temperature, the predicted ignition distance indicates that ignition is feasible within practical supersonic combustion engines. For the latter situations, the ignition event is initiated by radical proliferation and hence runaway instead of thermal runaway. Furthermore, it was demonstrated that the use of the similarity Blasius velocity at the leading edge can generate a high temperature spot which is convected downstream and artificially facilitates ignition. This work was reported in Publication No. 1, which was appended in the Annual Report for 1995-96.

The second study was an asymptotic analysis of the ignition of the hydrogen/air supersonic mixing layer using reduced reaction mechanisms. Two distinct reduced mechanisms for the high-temperature and low-temperature regimes were used depending on the characteristic temperature of the reaction zone relative to the crossover temperature at which the reaction rates of the $H+O_2$ branching and termination steps are equal. Each regime also involves two distinct analyses for the hot-stream and the viscous-heating cases, depending on the relative dominance of external and internal ignition energy sources. These four cases were been analyzed separately, and it was shown that the present analysis successfully

describes the ignition process by exhibiting turning point and thermal runaway behavior in the low-temperature regime, and radical branching followed by thermal runaway in the high-temperature regime. Results for the predicted ignition distances were then mapped out over the entire range of parameters, showing consistent behavior with the previous one-step model analysis. Furthermore, it was demonstrated that ignition in the low-temperature regime is controlled by a large activation energy process, so that the ignition distance is more sensitive to its characteristic temperature than that in the high-temperature regime. The ignition distance was also found to vary non-monotonically with the system pressure in the manner of the well-known hydrogen/oxygen explosion limits, thereby further substantiating the importance of chemical chain mechanisms in this class of chemically-reacting boundary layer flows. This work was reported in Publication No. 2, which was appended in the Annual Report for 1995-96.

Further improvements in the reduced mechanisms were conducted, and ignition in the counterflow has been studied. The first study was concerned with ignition in the high pressure situations of the third limit. In the analysis, simplifications to the chemical mechanism were formally derived, and criteria determining the accuracy of these simplifications were identified. It was demonstrated that the chemical steady-state approximations of O and OH are accurate for a wide range of conditions, while the steady-state approximations of H and HO_2 were both found to be inaccurate in certain regimes. Using these approximations, a reduced mechanism was derived and used to explain the ignition behavior of H_2 and O_2. It was shown that, for both the premixed and nonpremixed configurations, ignition occurs through the effect of heat release on the Arrhenius term of reaction $H_2O_2 + M \rightarrow 2OH + M$, and expressions were derived which were able to qualitatively predict the relationship between the pressure, temperature, and strain rate at ignition. The difference in ignition temperature between the premixed and nonpremixed configurations is associated with the effect of reactions between H and HO_2. For the premixed case, the rate of destruction of H through $H+O_2+M \rightarrow HO_2+M$ is much slower due to the lower concentration of O_2 in the reactions zone, thus reactions between H and HO_2 play a greater role in the ignition process. This work was reported in Publication No. 3, and attached herein as Appendix A.

A second analysis was performed for the situations of high temperature and low pressure. Starting with seven elementary reactions, a reduced mechanism was derived assuming steady state for the O and OH radicals. An algebraic ignition criterion was derived using this mechanism. This criterion successfully explains the

behavior analogous to the first and second explosion limits. A bifurcation analysis was then performed to clarify the ignition behavior. This analysis demonstrated that an ignition turning point can occur solely through the interaction of radical species with no contribution from heat release. The source of this turning was found to be the reaction $H + HO_2 \rightarrow 2OH$, confirming results from numerical calculations. The regimes in which abrupt or monotonic transition to an ignited state were re-calculated including the effect of this reaction. This work was reported in Publication No. 4, which is attached herein as Appendix B.

Publications

1. "A numerical study of ignition in the supersonic hydrogen/air laminar mixing layer," by M. Nishioka and C.K. Law, *Combustion and Flame*, Vol. 108, pp. 199-219 (1997).
2. "Ignition in the supersonic hydrogen/air mixing layer with reduced mechanisms," by H.G. Im, B.T. Helenbrook, S.R. Lee and C.K. Law, *Journal of Fluid Mechanics*, Vol. 322, pp. 275--296 (1996).
3. "Ignition of hydrogen and oxygen in counterflow at high pressures," by B.T. Helenbrook and C. K. Law, Twenty-Sixth Symposium (International) on Combustion, The Combustion Institute, Pittsburgh, PA. pp. 815-822 (1997). [Appendix A].
4. "Theory of thermal- and radical-induced ignition of counterflowing hydrogen versus oxygen at high temperatures," by B.T. Helenbrook, H.G. Im and C.K. Law, Combustion and Flame, in press. [Appendix B].

Presentation

"A Numerical Study of Ignition in the Supersonic Hydrogen/Air Laminar Mixing Layer," 33rd Aerospace Sciences Meeting, Reno, NV, Jan. 9-12, 1995.

Personnel

B.T. Helenbrook (Graduate student); will graduate by end of 1997.

Honors and Awards

1. 1997 Heat Transfer Memorial Award of the ASME.
2. Appointed Deputy Editor of *Combustion and Flame.*

Interactions and Inventions

None

APPENDIX A

Twenty-Sixth Symposium (International) on Combustion/The Combustion Institute, 1996/pp. 815–822

IGNITION OF HYDROGEN AND OXYGEN IN COUNTERFLOW AT HIGH PRESSURES

B. T. HELENBROOK AND C. K. LAW
Department of Mechanical and Aerospace Engineering
Princeton University, Princeton, NJ 08544

Ignition of hydrogen and oxygen in the "third limit" was studied in counterflow for both premixed and nonpremixed systems with activation energy asymptotics. The results of the analysis were then compared to numerical calculations for further verification of the findings. In the analysis, simplifications to the chemical mechanism were formally derived, and criteria determining the accuracy of these simplifications were identified. It was demonstrated that the chemical steady-state approximations of O and OH are accurate for a wide range of conditions, while the steady-state approximations of H and HO_2 were both found to be inaccurate in certain regimes. Using these approximations, a reduced mechanism was derived and used to explain the ignition behavior of H_2 and O_2. It is shown that, for both the premixed and nonpremixed configurations, ignition occurs through the effect of heat release on the Arrhenius term of reaction 15, $H_2O_2 + M \rightarrow 2OH + M$, and expressions were derived that are able to qualitatively predict the relationship between the pressure, temperature, and strain rate at ignition. The difference in ignition temperature between the premixed and nonpremixed configurations is associated with the effect of reactions between H and HO_2. For the premixed case, the rate of destruction of H through $H + O_2 + M \rightarrow HO_2 + M$ is much slower due to the lower concentration of O_2 in the reaction zone, thus reactions between H and HO_2 play a greater role in the ignition process.

Introduction

Hydrogen-oxygen combustion is of interest because it plays an underlying role in the combustion of all hydrocarbon fuels and because hydrogen is a practical fuel. This interest has motivated a substantial amount of research on its oxidation and combustion characteristics. Indeed, work done by Lewis and von Elbe [1], Baldwin and Mayer [2], Baulch et al. [3], Warnatz [4], and Yetter et al. [5] has resulted in a reliable description of the chemical kinetics of hydrogen oxidation, which has enabled further studies of the behavior of hydrogen-oxygen mixtures in various physical environments [6–8]. The counterflow mixing configuration has been extensively adopted for experimental, numerical, and analytical studies of hydrogen-oxygen combustion [9–14] because it embodies many of the physical processes seen in practical applications. Results from such studies have been able to assess the interaction of chemistry with convection and diffusion.

Numerical and experimental studies of hydrogen-oxygen ignition in the counterflow configuration have mapped the response of the system over a wide range of conditions for both premixed and nonpremixed systems. Similar to the homogeneous explosion limits of hydrogen-oxygen mixtures, three distinct ignition limits in such heterogeneous, mixing-affected systems were found [11]. In the first limit, ignition is governed by a balance between branching and diffusive loss of H, while the second limit is determined by a balance between branching and destruction of H through $H + O_2 + M \rightarrow HO_2 + M$. In the third limit, the branching rate of the hydrogen radical is not sufficiently fast to cause ignition, and ignition proceeds through a path involving hydrogen peroxide. In addition, numerical simulations have led to the suggestion of various skeletal mechanisms and simplified global mechanisms applicable to each limit [9,11].

For nonpremixed ignition, asymptotic analyses have been performed in the first and second limits [12–14] as well as the third limit [12]. The analysis of Ref. 12 for the third limit, however, was based on a reduced mechanism obtained from empirical observations of numerical results. As such, only limited insight was obtained. Therefore, the primary objective of the present investigation is to provide a rigorous and comprehensive analysis of the third ignition limit, for both premixed and nonpremixed systems, and through this analysis gain fundamental understanding of the ignition process. In this analysis, we will derive a global mechanism from a reduced set of reactions that has been shown to accurately predict ignition temperatures by previous numerical work [9,11] and has also been extensively tested in the course of the present investigation for both premixed and nonpremixed systems. By deriving the global mechanism asymptotically, we can find criteria governing the accuracy of this mechanism,

and thus avoid some of the inadequacies that can be associated with determining the mechanism strictly from numerical results. The formulation and various aspects of the analysis are sequentially presented in the following.

Formulation

Ignition of H_2-O_2 will be studied in the counterflow configuration. We are especially interested in finding a relation between the strain rate and the temperature and pressure of the flow at the point of ignition. Two distinct cases will be considered. In the first, the nonpremixed case, a cold jet of inert-diluted H_2 impinges on a hot jet of air. In the second, the premixed case, a cold jet of premixed H_2 and O_2 impinges on a hot inert jet. Due to similarities in the ignition behavior between these two cases, the analysis for both can be considered in parallel.

We will use numerical results to guide the asymptotic analysis and to verify its findings. These results have been calculated using a Newton iteration technique developed by Kee et al. [15] and modified for the counterflow configuration by Nishioka et al. [16]. This code solves a quasi-one-dimensional problem based on the similarity approximation. The calculations were done using mixture-averaged diffusion coefficients, potential flow boundary conditions, and the reaction mechanism given by Ref. 5.

For simplifications, we shall assume that the flow is potential described by $\rho v = (-\rho_\infty a\hat{x}\sigma,\ \rho_\infty a r)$, where $\hat{x}$ is the coordinate normal to the stagnation plane, ρ_∞ the density of the hot stream, a the strain rate of the flow, and $\sigma = 1, 2$ for planar and axisymmetric flows, respectively. Furthermore, c_p, λ, and ρD_i for all species were taken to be constants, while the Lewis numbers for all species were assumed to be unity except for H_2 and H, for which the values of 0.3 and 0.2 were used. With the above approximations, the governing equations in the nondimensional spatial coordinate, $\hat{x}/\sqrt{\lambda/c_p\rho_\infty a}$, become:

$$x\frac{dT}{dx} + \frac{d^2T}{dx^2} = -\frac{\bar{W}_\infty}{p_\infty a\sigma}\sum_m q_m\omega_m \tag{1}$$

$$x\frac{dY_i}{dx} + \frac{1}{Le_i}\frac{d^2Y_i}{dx^2} = -\frac{\bar{W}_\infty}{\rho_\infty a\sigma}\sum_m (v''_{i,m} - v'_{i,m})\omega_m \tag{2}$$

where $T = c_p\hat{T}\bar{W}_\infty/Q$, $Y_i = \hat{Y}_i\bar{W}_\infty/W_i$, and $q_m = \Sigma_i(v'_{i,m} - v''_{i,m})\hat{h}_i^\circ/Q$.

For nonpremixed ignition, the boundary conditions were set to describe air flowing against a mixture of H_2 and N_2.

$$\begin{aligned} &T = T_\infty, \quad Y_{O_2} = Y_{O_2,\infty} \\ &Y_i = 0\ (i \neq O_2, N_2); \quad x \to \infty \\ &T = T_\infty - \beta, \quad Y_{H_2} = Y_{H_2,-\infty} \\ &Y_i = 0\ (i \neq H_2, N_2); \quad x \to -\infty \end{aligned} \tag{3}$$

where $\beta = T_\infty - T_{-\infty}$. Furthermore, we shall use $Y_{H_2,-\infty} = 0.1$ and $\hat{T}_{-\infty} = 300$ K in the calculations. For premixed ignition, a mixture of oxygen and hydrogen flows against a stream of nitrogen, and only the boundary conditions for oxygen and nitrogen were changed so that for $x \to \infty$, $Y_{O_2} = 0$ and for $x \to -\infty$, $Y_{O_2} = Y_{O_2,-\infty}$.

The frozen solutions T_f and $Y_{i,f}$ are given in the form $c_1 + c_2\text{erfc}(x\sqrt{Le_i/2})$, where c_1 and c_2 are chosen to satisfy the boundary conditions given above. This completes formulation of the problem. An analysis of the above equations and comparison of their predictions with the numerical results follows.

Large Activation Energy Approximations

The first step in the analysis is to identify the characteristic chemical rate at ignition. We will show that for both premixed and nonpremixed systems, the only consistent choice for this rate is that of reaction 15. Since this reaction has an activation energy that is much larger than the ambient thermal energy of the system, we expect the analysis to follow procedures developed for one-step large activation energy ignition problems [17].

Inserting $T = T_f + \varepsilon\phi$ in the Arrhenius term of reaction 15 reveals that the proper scale for ε is $RT_\infty^2/E_{a,15}$ and that the solution domain is divided into three asymptotic zones. Near the hot boundary, $T_\infty - T_f$ is less than $O(\varepsilon)$, and the Arrhenius term of reaction 15 is nearly constant. In the "reaction" zone, the fuel concentration is much larger than near the hot boundary, while the Arrhenius term decreases exponentially due to an $O(\varepsilon)$ decrease in the frozen temperature, and in the downstream zone, reaction 15 is essentially frozen.

Since the reaction zone is located where $T_\infty - T_f$ is of $O(\varepsilon)$, we can expand this relation to reveal that the physical coordinate in this zone can be expressed as $x = x_r + \xi/x_r$, where changes in the Arrhenius term with ξ are $O(1)$ and x_r is a moderately large number. Thus, reaction will occur near the hot stream boundary in a narrow zone of width $1/x_r$ around the location x_r. In Fig. 1, we have plotted the H_2O_2 production rate, the H_2O_2 mass fraction, and the temperature at ignition from the numerical results. Examining the figure reveals that H_2O_2 is produced in a relatively narrow zone near the hot stream boundary from which it diffuses and convects outward. In this figure, we have also shown the position and width of the reaction zone found from the asymptotic expression. This estimation agrees rather well with the numerical results which confirms that, typical of many combustion problems, the location of the reaction zone is determined by the sensitive nature of the reaction rate to temperature. This is true for both the premixed and nonpremixed problems.

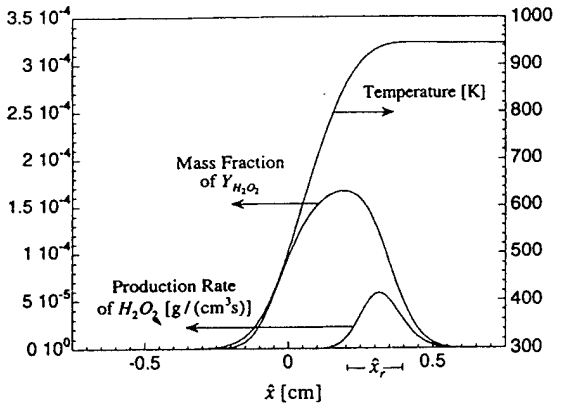

FIG. 1. Ignition profiles at a pressure of 5 atm and a strain rate of 10 s^{-1}.

Applying the above approximations, we can rewrite the governing equations in this zone as follows:

$$\frac{d\phi}{d\xi} + \frac{d^2\phi}{d\xi^2} = -\frac{\Delta}{\varepsilon}\sum_m q_m k_m Y_{m,1} Y_{m,2} \qquad (4)$$

$$\frac{dY_i}{d\xi} + \frac{1}{Le_i}\frac{d^2Y_i}{d\xi^2} = -\Delta \sum_m (\nu''_{i,m} - \nu'_{i,m}) k_m Y_{m,1} Y_{m,2} \qquad (5)$$

where

$$\Delta = \frac{\hat{k}_{15}(T_\infty)[C_M]}{\sigma a x_r^2} \quad \text{and}$$

$$k_m = \frac{\hat{k}_m(T_f)}{\hat{k}_{15}(T_\infty)} \exp(E_{a,m}\phi/E_{a,15}) \qquad (6)$$

These equations determine the ignition behavior for both the premixed and nonpremixed cases. In the above equations, Δ is the Damköhler number based on the convective-diffusive rate in the ignition zone and the rate of reaction 15. Since this reaction determines the characteristic chemical rate of ignition, we expect the Damköhler number to be $O(1)$ at ignition. Analysis of these equations will confirm this expectation, as well as determine the Damköhler number's dependence on the remaining parameters in the system.

Reaction Zone Chemistry

The next step in the analysis is to examine the chemistry occurring in the reaction zone. Examining the reactions in Table 1 reveals that several species are consumed at a rate that is much faster than the convective-diffusive rate in the ignition zone. The radicals O, OH, and H all fall into this category. Since consumption of these radicals occurs quickly, any radical produced will be consumed before diffusive loss can play a role in this process. Making the chemical steady-state approximation, we ignore the convective-diffusive terms and balance the chemical terms which gives an algebraic expression for the radical concentration.

For the O radical, the consumption reaction is reaction 2 which has a rate of $\Delta k_2 Y_{H_2 f}$ relative to the diffusive rate of the system. Sánchez et al. [14] have shown that for ignition in the first limit, the steady-state approximation of O is inaccurate. In the third limit, however, the characteristic ignition rate is much slower, and chemical steady-state of the O radical is an accurate approximation. The mass fraction of O, therefore, can be found by balancing the chemical production and destruction rates of O. Similarly for the OH radical, the rate of consumption through reaction 3 relative to the diffusive rate, $\Delta k_3 Y_{H_2 f}$, is $\gg 1$ such that this radical is also in steady state. Because the H_2 mass fraction in the reaction zone is

TABLE 1
Skeletal mechanism

No.	Reaction	A	n	E_a
R1	$H + O_2 \rightarrow OH + O$	1.92E + 14	0.00	16.44
R2	$O + H_2 \rightarrow OH + H$	5.08E + 04	2.67	6.29
R3	$OH + H_2 \rightarrow H_2O + H$	2.16E + 08	1.51	3.43
R9	$H + O_2 + M \rightarrow HO_2 + M$	6.17E + 19	−1.42	0.00
R10	$HO_2 + H \rightarrow H_2 + O_2$	6.63E + 13	0.00	2.13
R10b	$H_2 + O_2 \rightarrow HO_2 + H$	1.93E + 14	0.00	59.61
R11	$HO_2 + H \rightarrow 2OH$	1.69E + 14	0.00	0.87
R14	$HO_2 + HO_2 \rightarrow H_2O_2 + O_2$	3.02E + 12	0.00	1.39
R15	$H_2O_2 + M \rightarrow 2OH + M$	1.20E + 17	0.00	45.50
R17b	$HO_2 + H_2 \rightarrow H_2O_2 + H$	2.81E + 11	0.54	24.09

Units are mol, cm^3, s, K, and kcal; $k = AT^n \exp(-E_a/RT)$

the same for both the premixed and nonpremixed fuel streams, these approximations hold for both configurations.

Using these approximations in the reaction mechanism, we find the well known H branching path through reactions 1, 2, and 3, which occurs at a rate of $2k_1Y_HY_{O_2,f}$. In the third limit, this rate is slower than the consumption rate of H through reaction 9, $k_9Y_HY_{O_2,f}[C_M]$. Therefore, the combined result of these reactions is consumption of H at a rate of $2k_1(\kappa - 1)Y_{O_2,f}$ relative to the diffusive rate of the H radical, where κ is the ratio of the rate of reaction 9 to the branching rate, $k_9[C_M]/2k_1$, which depends on the pressure through $[C_M]$. Since k_1 is of $O(10^4 \sim 10^5)$, we expect the chemical steady-state approximation of H to be accurate when κ is larger than one and there is sufficient O_2 in the reaction zone. For the nonpremixed case, the O_2 mass fraction is $O(1)$ in the reaction zone, and this approximation is accurate even for pressures at which κ is nearly one. In the premixed configuration, the reaction zone is in the hot inert, and oxygen must diffuse into the reaction zone from the fuel stream. For $\kappa - 1$ of $O(1)$, the O_2 concentration in the reaction zone is enough to make the chemical steady-state approximation of H fairly accurate, but because the oxygen concentration rapidly decreases upstream of the reaction zone, convective-diffusive loss of the H radical may still have some influence. For larger κ, this influence is reduced, and the approximation becomes increasingly accurate.

Plotting the local destruction rate of these radicals along with their convective-diffusive rate, as in Ref. 11, verifies the accuracy of these approximations. Figure 2 was generated from the numerical results for a premixed fuel stream at a pressure of 7.4 atm, a strain rate of 13 s^{-1} and at a temperature of 1020 K which is within 1 K of the ignition point. At these conditions, κ is approximately 2.5. The figure shows that for the H radical, even for these near-worst-case conditions, the destruction rate is nearly ten times larger than the convective-diffusive rate, thus chemical production is mainly balanced by destruction. For the O and OH radicals, the destruction rates are more than an order of magnitude larger than the convective-diffusive rate, making the chemical steady-state approximation very accurate. This verifies that these approximations do predict the behavior of the numerical system.

We can use the preceding approximations to derive the following reduced mechanism which is valid only for ignition in the third limit:

Step I $$H_2O_2 + \frac{2\kappa + 1}{\kappa - 1}(H_2 + O_2) \rightarrow \frac{2\kappa}{k - 1}(HO_2 + H_2O)$$

Step II $$\frac{\kappa + 1/2}{\kappa - 1}(H_2 + O_2) \rightarrow H_2O_2 + \frac{1}{\kappa - 1}(HO_2 + H_2O)$$

Step III $$\frac{\kappa + 1/2}{\kappa - 1}H_2 + \frac{2\kappa - 1/2}{\kappa - 1}O_2 \rightarrow \frac{2\kappa - 1}{\kappa - 1}HO_2 + \frac{1}{\kappa - 1}H_2O$$

Step IV $$\frac{\kappa(4 - 2a) - (1 + a)}{2(\kappa - 1)}H_2 + \frac{\kappa(2 - 4a) + 1 + a}{2(\kappa - 1)}O_2 + \frac{2\kappa a - a - 1}{\kappa - 1}HO_2 \rightarrow \frac{2\kappa - a}{2(\kappa - 1)}H_2O$$

R14 $$HO_2 + HO_2 \rightarrow H_2O_2 + O_2$$

Steps I, II, and III occur at the rates of reactions 15, 17b, and 10b, respectively. Due to the branching of the H radical and consumption through reaction 9, each H or OH radical produced by these reactions results in the production of $\kappa/(\kappa - 1)$ HO_2 radicals. Step IV is the combined effect of reactions 11 and 10 where a is the ratio of the rates of these reactions, which is approximately 0.2. This reaction is relatively slow, and will be considered only as a correction to the leading order solution. Steps I, II, III, and reaction 14 determine the primary ignition mechanism of the system.

Ignition Mechanism

The remaining analysis focuses on the system evolution as the Damköhler number is increased to the turning point. To understand this evolution, we will begin by examining the behavior of the HO_2 radical. In the above reduced mechanism, HO_2 has two possible branching paths. The most apparent is through step II, which has a rate proportional to HO_2 and results in the production of $1/(\kappa - 1)$ HO_2 radicals. The second path is through a coupling of steps I and II. For pressures at which κ is moderately larger than one, this path is the faster route, and corresponds to the following pathway:

$HO_2 + H_2 \rightarrow H_2O_2 + H$	reaction 17b
$H_2O_2 + M \rightarrow 2OH$	reaction 15
$2OH + 2H_2 \rightarrow 2H + 2H_2O$	reaction 3
$3H + 3O_2 + 3M \rightarrow 3HO_2 + 3M$	reaction 9

(8)

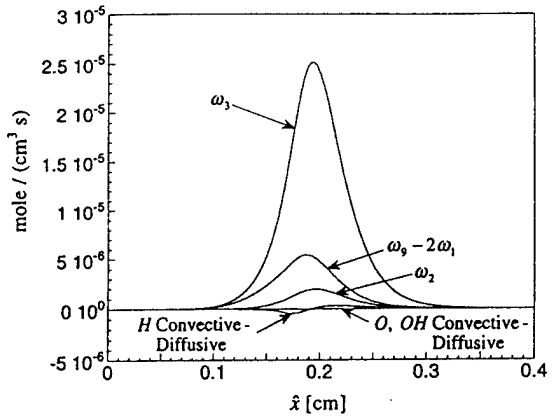

FIG. 2. Destruction rates and convective-diffusive rates of O, OH, and H at 7.4 atm, 13 s^{-1}, and 1020 K, which is within one degree of the ignition temperature.

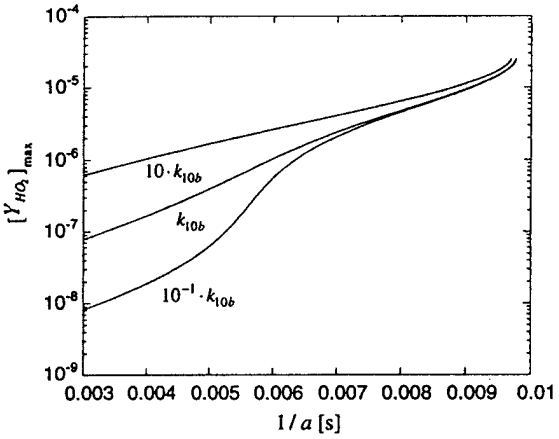

FIG. 3. Maximum HO_2 mass fraction versus $1/a$ for various initiation rates and a pressure and temperature of 5 atm and 970 K.

When the Damköhler number is of $O(\sqrt{(\kappa - 1)/(\kappa k_{15} k_{17b} Y_{H_2 f})})$, the branching rate of this path will be the same order as the convective-diffusive rate. For Damköhler numbers less than this value, the HO_2 concentration is determined mainly by a balance between the initiation reaction, R10b, and the convective-diffusive terms. For Damköhler numbers larger than this value, the rate of the branching reaction becomes faster than the convective-diffusive rate, and the HO_2 concentration increases to a level at which the dominant balance is between the production of HO_2 through this branching path and destruction of HO_2 by reaction 14. To verify this, the maximum mass fraction of HO_2 has been plotted versus $1/a$ for several initiation rates in Fig. 3. The calculations were performed at a pressure of 5 atm and a temperature of 970 K. At these conditions, the asymptotic expression predicts that at $1/a$ of order 0.004 s, the transition between these behaviors will occur. On the figure, the two regimes are identifiable. For $1/a$ less than approximately .007 s, the sensitivity to initiation is apparent while above this value, the maximum mass fraction, which typifies the variation of the profile in the reaction zone, becomes fairly insensitive to the different initiation rates. This confirms that the branching path is crucial in determining the HO_2 concentration at the ignition point.

For Damköhler numbers much larger than the value at which the branching increase of HO_2 takes place, we can neglect the convective-diffusive terms relative to the branching rate. This leads to the chemical steady-state approximation, $2w_{14} = [2\kappa w_{15} + w_{17b} + (2\kappa - 1)w_{10b}]/(\kappa - 1)$. Since the production rate of HO_2 through step I exceeds that from steps II and III, we can ignore the second two terms on the right-hand side of this equation and solve for the concentration of HO_2:

$$Y_{HO_2} = \sqrt{\frac{k_{15}\kappa}{k_{14}(\kappa - 1)}}\, Y_{H_2O_2} \tag{9}$$

For this expression to be correct, the Damköhler number at ignition must be much greater than that at which HO_2 branching first occurs.

Our final goal is to determine the mechanism that causes the ignition turning point. Using the previous findings we can rewrite the equations for H_2O_2 and ϕ:

$$\frac{dY_{H_2O_2}}{d\xi} + \frac{d^2Y_{H_2O_2}}{d\xi^2} = -\Delta\left[\frac{1}{\kappa - 1} k_{15} Y_{H_2O_2} + \frac{\kappa - 1/2}{\kappa - 1} k_{17b} Y_{H_2 f} \sqrt{\frac{k_{15}\kappa}{k_{14}(\kappa - 1)}}\, Y_{H_2O_2}\right] \tag{10}$$

$$\frac{d\phi}{d\xi} + \frac{d^2\phi}{d\xi^2} = -\frac{\Delta}{\varepsilon}\left[q_I k_{15} Y_{H_2O_2} + q_{II} k_{17b} Y_{H_2 f} \sqrt{\frac{k_{15}\kappa}{k_{14}(\kappa - 1)}}\, Y_{H_2O_2}\right] \tag{11}$$

Examining the above equations reveals that there are two sources for H_2O_2 and ϕ. The first is a branching path with a rate proportional to the concentration of H_2O_2. This path is simply step I followed by the conversion of HO_2 to H_2O_2 through reaction 14, and will cause a branching ignition when $\Delta/(\kappa - 1)$ is $O(1)$. The second path corresponds to step II with HO_2 converted to H_2O_2 by reaction 14. Because the rate of this path depends on the mass fraction of H_2O_2 to the one-half power, this path will only cause a quadratic increase in the concentration of H_2O_2 as the Damköhler number is increased. A turning point can occur only when the effect of heat release on the reaction rates is considered. Determining the amount of H_2O_2 produced by this path and inserting

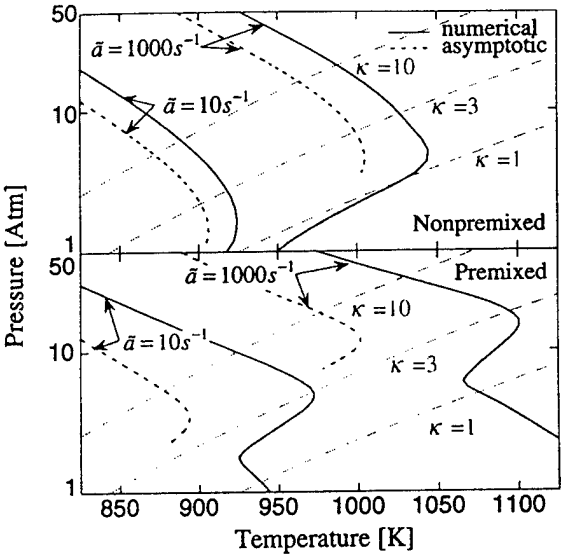

FIG. 4. Ignition pressure versus temperature for various density-weighted strain rates.

it into equation 11 results in the magnitude of the temperature perturbation. Both paths are important in determining the ignition Damköhler number, although the heat release from path I is larger. Using this path to determine an approximate scaling for the ignition Damköhler number, we arrive at the following expression:

$$\Delta_1 = \left[\frac{\varepsilon k_{14}(\kappa - 1)^3}{q_1\kappa(\kappa - 1/2)^2(k_{17b}Y_{H_2,r})^2}\right]^{1/3} \quad (12)$$

where the reaction rate constants are evaluated at T_∞, and $Y_{H_2,r}$ is the mass fraction in the reaction zone. Comparing this expression to the criterion for ignition through branching reveals that ignition through heat release occurs well before branching of H_2O_2 becomes important for all κ; therefore, heat release is the dominant ignition path. For $\kappa - 1$ of $O(1)$, this expression is an $O(1)$ quantity which confirms that reaction 15 determines the characteristic chemical rate at ignition. This is in agreement with the results found by Lee and Law [12] for κ much larger than one. However, we have now shown that for κ of $O(1)$, heat release is still dominant over the branching path in determining the ignition Damköhler number.

Using the leading-order scaling, we can also determine a correction of the form $\Delta = \Delta^0 + \Delta^1 \ldots$ caused by the effects of step IV. Assuming that the rate of reaction 11 is small, we arrive at the following correction to the heat release terms on the right-hand side of equation 11:

$$-\frac{\Delta^0\omega^0_{11}}{\varepsilon}\left[\frac{(-2\kappa\alpha + 1 + \alpha)}{(1 + \Delta^0)^2(2\kappa\Delta^0 + \Delta^0 + 1)}\right.$$
$$\left.\left(q_I\frac{\Delta^0(2\kappa\Delta^0 + \kappa)}{(\kappa - 1 - \Delta^0)} + q_{II}(1 + \Delta^0)\right) + q_{IV}\right] \quad (13)$$

from which we can determine the influence of step IV on the ignition Damköhler number. The first two terms in this expression result from the effect of step IV on the rates of steps I and II. The last term is the additional heat release derived from this step. Evaluating this expression, we have found that for most κ, the effect of reaction 11 on the rates of steps I and II is dominant over the heat release from this step. Near $\kappa = 3$, the effect on the reaction rates becomes very small because step IV neither produces nor destroys HO_2 at this κ. For $\kappa < 3$, because of the branching of the H radical, step IV actually begins to produce additional HO_2. The magnitude of this effect depends on the rate of reaction 11. Because the H radical concentration is inversely proportional to its consumption rate, $2k_1(\kappa - 1)Y_{O2,f}$, step IV will be much faster near $\kappa = 1$ than for large κ. In addition, since this rate is slower in the premixed configuration due to the lower oxygen concentration, step IV will have a greater influence on the premixed results. Therefore, this expression will explain some of the differences between the premixed and nonpremixed numerical results.

The final step in the analysis is to check that the steady-state approximation of HO_2 made previously is a valid approximation. To do this, we have calculated the ratio of the Damköhler number given by equation 12 to the Damköhler number found for HO_2 branching for various conditions. As previously mentioned, if this ratio is $\gg 1$, the branching rate of HO_2 is much faster than its convective-diffusive rate, and the chemical steady-state approximation is accurate. The results of these calculations reveal that this ratio is only between 2 and 10 for most conditions and that it decreases with increasing ignition temperature. Therefore, the chemical steady-state approximation is not very accurate, and convective-diffusive loss of the HO_2 radical is important in determining the ignition temperature, especially at high temperatures. However, as a first approximation, chemical steady-state of HO_2 still predicts the correct qualitative behavior.

Comparison to Numerical Results

In Fig. 4 we have plotted the ignition pressures and temperatures for various density-weighted strain rates calculated from the numerical results, along with the behavior predicted by equations 10 and 11, including the correction from expression 13. Here, instead of holding the strain rate, a, fixed, we hold $\rho_\infty a$ fixed, as in Ref. 11. $\tilde{a}$ is defined as the ratio of $\rho_\infty a$ to the value at $\kappa = 1$ for 1 atm. Holding $\tilde{a}$ constant is more appropriate because it fixes the scale of the problem, and thus isolates the chemical effects. On the plot, numerical calculations for both the premixed and nonpremixed configurations are shown. Examining the nonpremixed ignition results

reveals that the scaling from the asymptotic analysis predicts the ignition limits fairly well. At high pressures, the ignition limits are well predicted by balancing the chemical time of reaction 15 with the convective-diffusive time in the reaction zone as shown by equation 12. For κ approaching 1, the ignition temperature decreases due to the increased effect of the hydrogen branching path. Below $\kappa = 1$, the H radical is no longer in steady state, and the system transitions to the first limit behavior.

Examining the premixed ignition results, we see that the leading-order solution along with the correction from expression 13 does qualitatively predict the correct behavior. The difference in ignition temperature between the premixed and nonpremixed results can be understood by examining this correction. For large κ, the difference in ignition temperature between the premixed and nonpremixed results at constant κ is small, about 10 K. At these conditions, step IV is relatively slow because the large consumption rate of H causes its concentration to be low. As κ decreases, the difference in ignition temperature between the premixed and nonpremixed streams increases, reaching a maximum of nearly 100 K. This is again due to step IV. For decreasing κ, the H concentration increases, increasing the rate of this step and thus making ignition more difficult. For $\kappa < 3$, the ignition temperature of the premixed stream decreases with decreasing κ, rapidly approaching the ignition temperature of the nonpremixed stream. As previously mentioned, for $\kappa \approx 3$, step IV no longer consumes HO_2, but begins to produce HO_2. This along with the $O(1)$ effect of H branching on the ignition temperature results in the rapid decrease in ignition temperature as κ approaches one.

The premixed case shown in Fig. 4 also shows a relatively large discrepancy between the analytical and computational results near $\kappa = 1$. At these states, step IV becomes an $O(1)$ effect. Not only does this affect the leading-order analysis, but it also affects the steady-state approximation of H. Since reaction 11 is a branching path for H, branching through this path can exceed the consumption rate causing convective-diffusive loss of H to become important. For κ of $O(1)$, this effect results in the difference in ignition temperatures between the analysis and the numerical results, and as κ approaches 1, causes the transition to first limit behavior.

Conclusions

Ignition of counterflowing hydrogen and oxygen was studied asymptotically for ignition in the third limit, with the goal of understanding the ignition mechanism of this system. Because of the temperature-sensitive nature of reaction 15, we found that ignition occurs in a localized kernel near the high-temperature boundary. In addition, the analysis revealed that the radicals H, OH, and O are in chemical steady state because each is consumed at a rate that is much faster than the diffusive rate of the system. Using steady-state approximations for these radicals, a reduced mechanism was derived which simplified the remaining analysis. In analyzing the kinetics of HO_2, it was found that HO_2 has a branching path that when balanced with reaction 14 determines the concentration of HO_2 at the ignition point. Equations governing H_2O_2 and the temperature perturbation, ϕ, were derived which showed that in the third limit, ignition occurs through the effect of heat release on reaction 15, and were able to predict the dependence of the ignition temperature on strain rate and pressure for both nonpremixed and premixed fuel streams. The difference in ignition temperature between these two configurations was associated with the effect of reactions of H with HO_2. For the premixed configuration, the H concentration is much larger, such that reactions of H with other radical species has a greater influence on the ignition temperature.

Acknowledgment

The authors would like to acknowledge Dr. C. J. Sung for discussions and his help with the numerical calculations. This research was supported by the Army Research Office and the Air Force Office of Scientific Research.

REFERENCES

1. Lewis, B., and von Elbe, G., *Third Symposium on Combustion, Flames and Explosion Phenomena*, The Williams and Wilkins Company, Baltimore, 1949, pp. 484–493.
2. Baldwin, R. R., and Mayor, L., *Seventh Symposium (International) on Combustion*, Butterworths, London, 1959, pp. 8–15.
3. Baulch, D. L., Drysdale, D. D., Horne, D. G., and Lloyd, A. C., *Evaluated Kinetic Data for High Temperature Reactions*, Butterworths, London, 1972, Vol. 1.
4. Warnatz, J., *Combustion Chemistry* (W. C. Gardiner Jr., Ed.), Springer-Verlag, New York, 1984, pp. 197–360.
5. Yetter, R. A., Dryer, F. L., and Rabitz, H., *Combust. Sci. Technol.* 79:97–128 (1991).
6. Maas, U., and Warnatz, J., *Combust. Flame* 74:53–69 (1988).
7. Treviño, C., *Progress in Astronautics and Aeronautics* (A. L. Kuhl, J. C. Leyer, A. A. Borisov, and W. A. Sirignano, Eds.), AIAA, Washington DC, 1991, Vol. 131, pp. 19–43.

8. Vlachos, D. G., Schmidt, L. D., and Aris, R., *Combust. Flame* 95:313–335 (1993).
9. Balakrishnan, G., Smooke, M. D., and Williams, F. A., *Combust. Flame* 102:329–340 (1995).
10. Fotache, C. G., Kreutz, T. G., Zhu, D. L., and Law C. K., *Combust. Sci. Technol.* 109:373–394 (1995).
11. Kreutz, T. G. and Law, C. K., *Combust. Flame,* (1996), submitted.
12. Lee, S. R. and Law, C. K., *Combust. Sci. Technol.* 97:377–389 (1994).
13. Sánchez, A. L., Liñán, A., and Williams, F. A., *Twenty-Fifth Symposium (International) on Combustion,* The Combustion Institute, Pittsburgh, 1994, pp. 1529–1537.
14. Sánchez, A. L., Balakrishnan, G., Liñán, A., and Williams, F. A., *Combust. Flame* 105:569–590 (1996).
15. Kee, R. J., Grcar, J. F., Smooke, M. D., and Miller, J. A., *A Fortran Program for Modeling Steady Laminar One-Dimensional Flames,* Sandia National Laboratories Report No. SAND85-8240, 1985.
16. Nishioka, M., Law, C. K., and Takeno, T., *Combust. Flame,* 104:328–342 (1996).
17. Liñán, A., *Acta Astronautica* 1:1007–1039 (1974).

Theory of Thermal- and Radical-Induced Ignition of Counterflowing Hydrogen versus Oxygen at High Temperatures

B. T. Helenbrook, H. G. Im*, and C. K. Law
Department of Mechanical and Aerospace Engineering
Princeton University, Princeton, NJ 08544

Abstract

Ignition of hydrogen and oxygen in counterflow was studied using asymptotic methods for temperatures above the "crossover temperature". Starting from eight elementary reaction steps, a reduced mechanism was formally derived which revealed that ignition in the high temperature regime is characterized by a balance between branching, termination and transport of the hydrogen radical within the reaction zone. Additionally, an algebraic ignition criterion was derived which predicts the ignition state as a function of the parameters defining the system. This criterion successfully explains the behavior analogous to the "first" and "second" explosion limits observed in homogeneous hydrogen-oxygen mixtures. A bifurcation analysis was then performed to clarify the ignition behavior. It was found that there are three distinct sub-regimes of the high-temperature ignition regime. Specifically, at ignition pressures for which the rate of the termination reaction, $H+O_2+M \rightarrow HO_2+M$, is comparable to the branching rate, abrupt ignition occurs through the nonlinear effect of the reaction $H+HO_2 \rightarrow 2OH$ on the net branching rate. At moderately low pressures, production of HO_2 becomes negligible, and the HO_2 chemistry no longer controls the ignition process. At these pressures, abrupt ignition is caused by the effect of heat release on the branching rate. Finally, at very low pressures depletion of oxygen in the reaction zone prevents an abrupt ignition, and a monotonic transition to an ignited state occurs. The behavior predicted by the asymptotic analysis is in agreement with predictions from numerical calculations with full chemistry. In addition, the asymptotic analysis isolated the different physical mechanisms underlying the ignition behavior and determined parameters governing the transition between these mechanisms.

*Present address: Center for Turbulence Research, Stanford University, Stanford, CA 94305.

Introduction

Because hydrogen-oxygen combustion is of interest for its application in supersonic propulsion, for its fundamental role in hydrocarbon combustion, and for its potential as a clean burning energy source, there has been substantial research done on its oxidation and combustion characteristics. An extensive amount of work (Baulch *et al.*, 1972; Warnatz, 1984; Yetter *et al.*, 1991) has been performed on determining the elementary chemical mechanism which governs hydrogen oxidation, and has produced a reliable description of the associated oxidation kinetics. This chemical mechanism has since been used to study the behavior of hydrogen-oxygen combustion numerically in various physical configurations. Specifically, numerical investigations have been performed on homogeneous mixtures (Maas and Warnatz, 1988) and then extended to more complicated situations involving diffusive transport (Balakrishnan *et al.*, 1995; Darabiha and Candel, 1992; Kreutz *et al.*, 1994; Vlachos *et al.*, 1993). These investigations have shown that this chemical mechanism, although simple compared to most hydrocarbons, can produce surprisingly complex behaviors.

All of the previous studies have reported that an important parameter in hydrogen-oxygen ignition is the "crossover temperature", T^*. This is the temperature at which the hydrogen branching rate is equal to the recombination rate of the hydrogen radical with oxygen at a given pressure. For temperatures above T^*, the branching rate exceeds the termination rate, and ignition is governed by the fate of the hydrogen radical. For temperatures below T^*, the branching rate of the hydrogen radical is not sufficiently fast to cause ignition, and ignition takes place through an alternate path involving hydrogen peroxide. The crossover temperature therefore divides hydrogen-oxygen ignition into two distinct regimes each having its own unique behavior. This study will focus on ignition which occurs at temperatures greater than the crossover temperature.

Numerical and asymptotic studies of the high temperature regime have shown that the ignition behavior can vary depending on parameters such as the temperature, pressure, reactant concentration, and the physical geometry. For example, a numerical investigation of the counterflow configuration by Balakrishnan *et al.* (1995) has shown that for ignition temperatures much greater than T^*, abrupt ignition does not occur. Instead, a monotonic transition to a strongly burning state is observed. This unique behavior of high-temperature ignition has been further investigated in a bifurcation analysis by Sánchez *et al.* (1994). They have confirmed that when the temperature is sufficiently large, a supercritical bifurcation is observed as the Damköhler number increases, implying a monotonic transition to the strongly burning state. Furthermore, the analysis has also revealed that, as the temperature approaches the crossover value, thermal feedback changes the behavior from a supercritical to a subcritical bifurcation, and thus the conventional turning-point ignition is resumed. This study therefore suggests a more refined classification of the ignition behavior for high temperatures, depending on whether the temperature is high enough to suppress the effect of thermal feedback.

A numerical study of the same problem by Kreutz *et al.* (1994) has found that when the temperature of the hot air stream is moderately higher than T^*, the ignition turning-point is attained purely by a nonlinear coupling between radicals, without consideration of heat release. Specifically, this coupling is effected by an additional branching step $H + HO_2 \rightarrow 2OH$, and constitutes an additional sub-regime in the high-temperature ignition chemistry.

The present study attempts to resolve all of the possible factors that are responsible for these distinguishing ignition characteristics observed in high-temperature ignition. In doing so, we first notice that the previous asymptotic studies have either used reduced mechanisms which have assumed the steady-state approximation for the hydroperoxyl radical (Sánchez

et al. 1994) or omitted the elementary step $H + HO_2 \rightarrow 2OH$ from the reduced mechanism (Lee and Law, 1994), thereby ruling out the possibility of radical coupling observed by Kreutz *et al.* (1994). The present analysis, therefore, starts with the derivation of a reduced mechanism from eight elementary reaction steps based on asymptotics. Using this mechanism, we shall perform a bifurcation analysis analogous to that of Sánchez *et al.* (1994). By exploiting the asymptotic limit of small Lewis number for the hydrogen radical, we obtain a simple algebraic expression for the ignition criterion which elucidates the physical interpretation of the high-temperature ignition phenomena in terms of all system parameters. It is found that high-temperature hydrogen-oxygen ignition exhibits three distinct sub-regimes, namely radical-radical coupling, radical-thermal feedback, and monotonic transition, as the temperature increases from the crossover temperature. We shall also identify parameters governing the transitions between these three cases.

Formulation

The problem considered is a counterflow configuration in which a stream of cold hydrogen impinges on a hot stream of oxygen-nitrogen mixture. A potential flow solution is used to describe the flow field in which the mass flux is given by $\rho \mathbf{v} = (-\rho_o a \hat{x} \sigma, \rho_o a r)$. In this expression, $\hat{x}$ is the similarity coordinate normal to the stagnation plane, ρ_o is the density of the incoming oxidizer stream, a is the strain rate of the flow, and σ is a constant which is equal to one for planar flow and two for axisymmetric flow. We further assume constant and equal values of c_p for all species, and constant values of λ and ρD_i. Unity Lewis number for all species is also assumed except for H_2 and H, for which the value of 0.2 was used. Using the nondimensional spatial coordinate, $\hat{x}/\sqrt{D_H/a}$, the governing equations become:

$$x\frac{dT}{dx} + Le_H \frac{d^2T}{dx^2} = \frac{W_{O_2}}{\rho_o a \hat{Y}^o_{O_2} \sigma} \sum_m q_m \omega_m, \tag{1}$$

$$x\frac{dY_i}{dx} + \frac{Le_H}{Le_i}\frac{d^2Y_i}{dx^2} = -\frac{W_{O_2}}{\rho_o a \hat{Y}^o_{O_2}\sigma}\sum_m(\nu''_{i,m} - \nu'_{i,m})\omega_m, \tag{2}$$

where $\hat{Y}^o_{O_2}$ is the mass fraction of oxygen in the incoming oxidizer stream, $T = c_p\hat{T}W_{O_2}/Q\hat{Y}^o_{O_2}$, $Y_i = \hat{Y}_i W_{O_2}/\hat{Y}^o_{O_2}W_i$, $q_m = \sum_i(\nu''_{i,m} - \nu'_{i,m})h^o_i/Q$, and $\omega_m = \prod_\ell[\rho_o Y_{m,l}\hat{Y}^o_{O_2}/W_{O_2}]A_m T^{n_m}\exp(-T_{a,m}/T)$.

Equations (1) and (2) are subject to the following boundary conditions:

$$\begin{aligned} &T = T_\infty, \;\; Y_{O_2} = 1, \;\; Y_i = 0 \;(i \neq O_2, N_2); \;\; x \to \infty, \\ &T = T_\infty - \beta, \;\; Y_{H_2} = Y^o_{H_2}, \;\; Y_i = 0 \;(i \neq H_2, N_2); \; x \to -\infty, \end{aligned} \tag{3}$$

where $\beta = T_\infty - T_{-\infty}$ with $\hat{T}_{-\infty}$ maintained at 300K for this problem. When chemical reaction is frozen, the temperature, hydrogen, and oxygen mass fractions are described by:

$$\begin{aligned} T_f = T_\infty - \frac{\beta}{2}\mathrm{erfc}(x/\sqrt{2Le_H}), \;\; Y_{H_2,f} = \frac{Y^o_{H_2}}{2}\mathrm{erfc}(x/\sqrt{2}), \text{ and} \\ Y_{O_2,f} = 1 - \frac{1}{2}\mathrm{erfc}(x/\sqrt{2Le_H}), \end{aligned} \tag{4}$$

which will be used as the basic solution for the asymptotic analysis to be presented in the next section. We remark that the boundary conditions are applied at finite distances away from the stagnation plane and are taken to the limit of large distances. This is to avoid mathematical difficulties arising from imposing the boundary conditions at infinity.

To proceed with the analysis, we need to define the chemical mechanism of hydrogen oxidation. This mechanism is adequately described by considering eight species and nineteen reversible reactions (Yetter *et al.*, 1991). Numerical results (Treviño, 1991; Kreutz and Law, 1993) have shown that at temperatures above T^*, the eight elementary reaction steps shown in table 1 adequately determine the ignition behavior. Hydrogen peroxide does not play a role in this mechanism because at temperatures greater than T^*, H_2O_2 reactions are too slow to influence the ignition process. Once the problem is solved one can easily verify that the neglected reactions have negligible rates.

Asymptotic Analysis and Results

Anticipating that the ignition process is governed by the fate of the hydrogen radical, we normalize the reaction rate constants in the problem by the rate constant of the branching reaction, R1, at T_∞. Since at ignition only small perturbations to the frozen solutions are expected, we expand the temperature as $T = T_f + \phi$, where $\phi \ll T_f$. This results in governing equations of the form:

$$x\frac{d\phi}{dx} + Le_H\frac{d^2\phi}{dx^2} = \Delta\sum_m q_m k_m Y_{m,1}Y_{m,2}, \tag{5}$$

$$x\frac{dY_i}{dx} + \frac{Le_H}{Le_i}\frac{d^2Y_i}{dx^2} = -\Delta\sum_m(\nu''_{i,m} - \nu'_{i,m})k_m Y_{m,1}Y_{m,2}, \tag{6}$$

where

$$\Delta = \frac{\rho^2\hat{Y}^\circ_{O_2}}{\sigma\rho_\circ a W_{O_2}}A_1\exp(-T_{a,1}/T_\infty),$$

$$k_m = \frac{A_m}{A_1}T_f^{n_m}\exp(T_{a,1}/T_\infty - T_{a,m}/T_f)\exp(T_{a,m}\phi/T_f^2), \quad \text{for } m \neq 9, \tag{7}$$

$$k_9 = \frac{\rho_f}{W_{mix}}\frac{A_9}{A_1}T_f^{n_9}\exp(T_{a,1}/T_\infty).$$

We note that the normalized rate constants are a function of the frozen temperature, T_f, and the temperature perturbation, ϕ. Δ is the Damköhler number based on the hydrogen branching rate and the characteristic convective rate of the system. At ignition, we expect this ratio to be $O(1)$.

Examining the equation governing the oxygen radical, we insert perturbations to the frozen reactant concentrations of the form $Y_{O_2} = Y_{O_2,f} - y_{O_2}$ and $Y_{H_2} = Y_{H_2,f} - y_{H_2}$, where y_{O_2} and y_{H_2} are expected to be small compared to their respective frozen values. This results in the following equation for Y_O:

$$\begin{aligned} x\frac{dY_O}{dx} + Le_H\frac{d^2Y_O}{dx^2} = -\Delta[&k_1 Y_H(Y_{O_2,f} - y_{O_2}) \\ &-k_2(Y_{H_2,f} - y_{H_2})Y_O - k_{12}Y_{HO_2}Y_O]. \end{aligned} \tag{8}$$

The coefficient of Y_O in the reaction mechanism, $k_2 Y_{H_2,f}$, is $\gg 1$ for $O(1)$ x and $O(1)$ mass fractions of H_2 in the fuel stream. Therefore the rate

of reaction 2 will be much larger than the convective-diffusive rate for any scale of Y_O. As a first approximation, we can neglect the convective and diffusive terms and put the oxygen radical in chemical steady state. This leads to the following expression for Y_O:

$$Y_O = \frac{k_1 Y_H (Y_{O_2,f} - y_{O_2})}{k_2 (Y_{H_2,f} - y_{H_2}) + k_{12} Y_{HO_2}}. \tag{9}$$

This approximation breaks down for large positive x where $Y_{H_2,f}$ becomes $O(1/k_2)$. The second order correction to this approximation in the reaction mechanism is of $O(Y_H/k_2 Y_{H_2,f})$ which is negligible compared to the branching rate.

In a similar manner, we can write the governing equation for the mass fraction of Y_{OH}:

$$\begin{aligned} x\frac{dY_{OH}}{dx} + Le_H \frac{d^2 Y_{OH}}{dx^2} = -\Delta \left[k_1 Y_H (Y_{O_2,f} - y_{O_2}) + k_2 (Y_{H_2,f} - y_{H_2}) Y_O \right. \\ \left. - k_3 (Y_{H_2,f} - y_{H_2}) Y_{OH} + 2k_{11} Y_H Y_{HO_2} + k_{12} Y_{HO_2} Y_O \right] \end{aligned} \tag{10}$$

The coefficient of Y_{OH} in the reaction mechanism, $k_3 Y_{H_2,f}$, is much larger than one for x of $O(1)$, so we can again assume OH to be in chemical steady state, with $\omega_3 = \omega_1 + \omega_2 + 2\omega_{11} + \omega_{12}$. These approximations considerably reduce the complexity of the problem because all occurrences of Y_O and Y_{OH} in the reaction mechanism can be eliminated. Differential equations need to be solved only for the remaining species.

To proceed with the analysis, the governing equations were put in linear form in a manner similar to that of Sánchez *et al.* (1994). Inserting expansions of the form:

$$\begin{aligned} Y_H = \epsilon y_{H,1} + \epsilon^2 y_{H,2}, \quad Y_{HO_2} = \epsilon y_{HO_2,1}, \quad Y_{H_2} = Y_{H_2,f} - \epsilon y_{H_2,1}, \\ Y_{O_2} = Y_{O_2,f} - \epsilon y_{O_2,1}, \quad \phi = \epsilon \phi_1, \quad \Delta = \Delta_I + \epsilon \Delta_B, \end{aligned} \tag{11}$$

and gathering terms of like order in ϵ, the governing equations become at $O(\epsilon)$:

$$x\frac{dy_{H,1}}{dx} + \frac{d^2 y_{H,1}}{dx^2} = -\Delta_I (2k_{1,f} - k_{9,f}) Y_{O_2,f} y_{H,1}, \tag{12}$$

$$x\frac{dy_{HO_2,1}}{dx} + Le_H\frac{d^2y_{HO_2,1}}{dx^2} = -\Delta_I k_{9,f} Y_{O_2,f} y_{H,1}, \tag{13}$$

$$x\frac{dy_{O_2,1}}{dx} + Le_H\frac{d^2y_{O_2,1}}{dx^2} = -\Delta_I (k_{1,f} + k_{9,f}) Y_{O_2,f} y_{H,1}, \tag{14}$$

$$x\frac{d\phi_1}{dx} + Le_H\frac{d^2\phi_1}{dx^2} = \Delta_I (q_1^* k_{1,f} + q_9 k_{9,f}) Y_{O_2,f} y_{H,1}, \tag{15}$$

$$x\frac{dy_{H_2,1}}{dx} + \frac{d^2y_{H_2,1}}{dx^2} = -3\Delta_I k_{1,f} Y_{O_2,f} y_{H,1}, \tag{16}$$

and at $O(\epsilon^2)$:

$$\begin{aligned} x\frac{dy_{H,2}}{dx} + \frac{d^2y_{H,2}}{dx^2} &= -\Delta_B (2k_{1,f} - k_{9,f}) Y_{O_2,f} y_{H,1} \\ &-\Delta_I \left[2k_{1,f} \left(y_{H,2} Y_{O_2,f} + Y_{O_2,f} \frac{T_{a,1}}{T_f^2} \phi y_{H,1} - y_{H,1} y_{O_2,1} - y_{H,1} Y_{O_2,f} \frac{k_{12,f} y_{HO_2,1}}{k_{2,f} Y_{H_2,f}} \right) \right. \\ &\left. -k_{9,f} (y_{H,2} Y_{O_2,f} - y_{H,1} y_{O_2,1}) + k_{11,f} \left(1 - \frac{k_{10,f}}{k_{11,f}} \right) y_{HO_2,1} y_{H,1} \right], \end{aligned} \tag{17}$$

where $q_1^* = q_1 + q_3 + 2q_3$ and $k_{m,f}$ is the rate constant of reaction m evaluated at the frozen temperature. The $O(\epsilon)$ equations determine the ignition Damköhler number, Δ_I, while the $O(\epsilon^2)$ equation for the hydrogen radical, Eq. (17), determines the behavior of the ignition point, Δ_B. The meaning of the bifurcation factor, Δ_B, will be discussed in a subsequent section.

The first order equations are equivalent to those which would result from applying the chemical steady state assumption of the O and OH radicals to reactions 1, 2, 3, and 9:

$$\begin{aligned} 3H_2 + O_2 &\rightarrow 2H + 2H_2O \quad \omega = \omega_1, \\ H + O_2 + M &\rightarrow HO_2 + M \quad \omega = \omega_9. \end{aligned} \tag{18}$$

This mechanism clearly shows the importance of the crossover temperature defined by $2k_1 = k_9$. For $T_\infty > T^*$, the H production rate is greater than its termination rate, and a chain branching explosion is possible. For $T_\infty < T^*$, chain branching explosion of H can no longer occur, and ignition must proceed through a different chemical process. The preceding reduced mechanism is the most fundamental mechanism which can be used to determine the hydrogen-oxygen ignition limits for temperatures above the crossover temperature.

The first order equation for the hydrogen radical, Eq. (12), is a linear eigenvalue problem which determines the ignition Damköhler number. The initiation reaction, R10b, has been neglected in this equation. Because of its slow rate, this reaction will only be important on the slowly burning branch of the solution. Since Eq. (12) is an eigenvalue problem, adding or subtracting a small source term such as initiation changes only the behavior of the solution up to the ignition point; the ignition Damköhler number remains unaffected. To confirm this, figure 1 compares the maximum value of Y_H determined from the numerical solution of Eq. (12) with various initiation rates to the case in which initiation has been neglected. The behavior shows that neither the ignition Damköhler number nor the behavior of the solution above the ignition point is affected by order of magnitude changes in the initiation rate. After ignition occurs, the sharp increase in the hydrogen radical concentration causes the rate of the branching reaction to be orders of magnitude greater than the initiation reaction. We can therefore ignore the effect of the initiation reaction in determining Δ_I and the behavior of the solution at the turning point.

Another point to note is that the frozen fuel concentration does not appear in the first order equations. This results from the steady state approximation of the O and OH radicals. Because the rate constants of reactions 2 and 3 are much greater than that of reaction 1 these reactions do not limit the ignition process. Since these are the only reactions dependent on the fuel concentration, Δ_I is independent of the H_2 concentration. This is in agreement with numerical calculations which show that the pressure and temperature ignition limits are insensitive to the H_2 concentration (Balakrishnan *et al.*, 1995).

Similarly, the higher order perturbation, y_{H_2}, was also neglected in Eq. (17). Depletion of H_2 in the reaction zone will have a weak effect on the ignition behavior because of the weak dependence on the H_2 concentration in the first order equations. The effect of hydrogen depletion in the reaction

zone is captured only for frozen H_2 concentrations small enough to cause departure from the chemical steady state approximations.

Ignition Criterion

In proceeding with the asymptotic analysis to determine the ignition criterion, two possible limiting processes can be exploited. First, we can pursue the large activation energy limit, which is commonly used in problems with one-step chemistry (e.g. Liñán, 1974). However, due to the large diffusivity of the hydrogen radical, it becomes difficult to match solutions between the various asymptotic zones (See Appendix A). To avoid this difficulty, we instead use the Lewis number of the hydrogen radical as a small expansion parameter as in Sánchez *et al.* (1994). When the Lewis number is treated as a small parameter, we find that the solution domain is divided into three zones. In a zone of width $O(\sqrt{Le_H})$ around the stagnation plane, the frozen temperature profile decays from T_∞ to $T_{-\infty}$ and the frozen oxygen profile decays from one to zero. Upstream of the stagnation plane in the oxygen jet, the temperature and oxygen mass fraction are constant equal to T_∞ and 1 respectively. Similarly in the hydrogen jet, the temperature and oxygen mass fraction are constant equal to $T_{-\infty}$ and 0 respectively. A schematic of the asymptotic structure is shown in figure 2. Ignition is expected to occur in the high temperature stream due to the non-zero oxygen concentration and the exponentially larger reaction rates in the high temperature stream.

A difficulty in the analysis is that equations (12)-(17) are not valid for $x \gg 1$ due to the breakdown of the steady state approximations. To match the solution to the high temperature boundary through this zone, two limiting approaches were used. The first approach assumed that the chemical steady state approximations remain valid to the upstream boundary. This method overestimates the reaction rates in this zone and thus gives a lower limit to the ignition Damköhler number. The second method assumed that reaction was frozen for some $x \gg 1$. These two methods give

suitable bounds to the influence of reaction in the large x zone on the ignition Damköhler number. Appendix B compares the difference between these two approaches. We found that if the steady state assumptions hold for $x \gg 1$ then the difference between these two approaches is negligible.

The equation for $y_{H,1}$ is uncoupled from the equations governing the remaining species, and is solely responsible for determining the ignition Damköhler number. Inserting expansions of the form $\Delta_I = \Delta_I^{(1)} + \sqrt{Le_H}\Delta_I^{(2)} + Le_H\Delta_I^{(3)} \ldots$ and $y_{H,1} = y_{H,1}^{(1)} + \sqrt{Le_H}y_{H,1}^{(2)} + Le_H y_{H,1}^{(3)} \ldots$ into equation (12) and matching, we were able to find an analytic expression for Δ_I. To first order, Y_H simply diffuses through the inner zone, and as we expected, the ignition criterion is determined by the chemistry in the high temperature stream. The first order expression for Δ_I is given by:

$$\sqrt{\pi} = -\Gamma\left(\frac{1-(2k_{1,\infty}-k_{9,\infty})\Delta_I^{(1)}}{2}\right)/\Gamma\left(1-\frac{(2k_{1,\infty}-k_{9,\infty})\Delta_I^{(1)}}{2}\right), \quad (19)$$

where $k_{1,\infty}$ and $k_{9,\infty}$ are equal to k_1 and k_9 evaluated at T_∞, and Γ is the gamma function. Given that $k_{1,\infty}$ is equal to one, $\Delta_I^{(1)}$ can be calculated to be $1.425/(2-k_{9,\infty})$. Thus for $O(1)$ values of the effective branching rate, $(2-k_{9,\infty})$, the ignition Damköhler number is $O(1)$ as we anticipated. However, for smaller effective branching rates Δ_I can become $\gg 1$. As Δ_I becomes large, the effect of reactions which initially had very slow rates will be amplified and cause the analysis to breakdown. Indeed, this is how the transition to the third ignition limit occurs. Peroxyl path reactions become important, and ignition no longer occurs simply through hydrogen radical branching. Transition to the third limit is not captured by this analysis.

Further matching resulted in an integral expression for $\Delta_I^{(2)}$ which was simplified using the activation energy as a large expansion parameter:

$$\Delta_I^{(2)} = \frac{\sqrt{2\pi}\Delta_I^{(1)}(2-k_{9,\infty})}{\Psi\left(\left[1-(2-k_{9,\infty})\Delta_I^{(1)}\right]/2\right)-\Psi\left(1-(2-k_{9,\infty})\Delta_I^{(1)}/2\right)}\frac{2x_r}{(2-k_{9,\infty})^2}, \quad (20)$$

where Ψ is the digamma function and x_r is determined from the relation $\exp(-x_r^2/2)/\sqrt{2\pi}x_r = T_\infty^2/T_{a,1}\beta$. Physically, x_r is the location of the ex-

ponential decay of the branching rate due to the temperature gradient, in nondimensional lengths of $\sqrt{\lambda/\rho_o c_p a}$. The source of this correction can be attributed to the exponential decay of the branching rate at $\sqrt{Le_H}x_r$ instead of at the stagnation plane as the first order analysis assumes.

Combining the previous expressions results in:

$$\Delta_I = \frac{1.425}{(2-k_{9,\infty})} + \frac{0.97\sqrt{Le_H}x_r}{(2-k_{9,\infty})^2} + O(Le_H). \tag{21}$$

This expression has been compared to the ignition Damköhler number calculated from equation (12) numerically and found to be accurate to within 3% over most of the parameter range. We can explain some fundamental properties of hydrogen-oxygen ignition using this expression. Rewriting it in terms of dimensional quantities gives:

$$2\frac{\rho_o \hat{Y}^o_{O_2}}{W_{O_2}} A_1 e^{-T_{a,1}/T_\infty} - \frac{\rho_o^2 \hat{Y}^o_{O_2}}{W_{air} W_{O_2}} A_9 T_\infty^{n_9} = a\sigma(1.425 + \frac{0.97\sqrt{Le_H}x_r}{2-k_{9,\infty}}). \tag{22}$$

This expression clearly shows that hydrogen-oxygen ignition at temperatures above the crossover temperature is determined by a balance between branching and termination of the hydrogen radical in the high temperature stream with a convective-diffusive loss term which is proportional to the strain rate.

Using this ignition criterion, we can determine the ignition pressure as a function of T_∞ for a given strain rate, as shown in figure 3. These curves behave in a manner analogous to the "first" and "second" limits of the homogeneous hydrogen-oxygen system. In the first limit, the pressure is low such that the termination rate, R9, which is a three body reaction, becomes slow relative to the branching reaction, R1. In equation (22), we can ignore the termination term and the equation reduces to $\rho_o \exp(-T_{a,1}/T_\infty) = constant$. Therefore in the first limit, for a constant strain rate a decrease in pressure must be accompanied by an increase in temperature. In the second limit, the branching and termination rates nearly balance so we can write $2A_1 \exp(-T_{a,1}/T_\infty) = \rho_o A_9 T_\infty^{n_9}/W_{Air}$, which is simply the expression for the

crossover temperature. This limit is insensitive to variations in the strain rate due to the small net branching rate, $(2 - k_{9,\infty})$. This can be seen by taking the derivative of the first order expression for Δ_I:

$$\frac{dD}{d\Delta_I} = -\frac{D^2}{1.425}, \tag{23}$$

where D is the net branching rate, $(2 - k_{9,\infty})$. In the second limit, the net branching rate is small, therefore large changes in the strain rate can be balanced by small changes in the net branching rate.

The ignition pressures and temperatures predicted by this expression show good qualitative agreement with the numerical calculations using full chemistry. However, the ignition temperatures are as much as 80K below the numerical ignition temperatures (Kreutz and Law, 1995). The difference could possibly be attributed to simplifications such as the assumption of constant transport coefficients, or assumptions regarding Le_i or c_p. In any case, the real value of the asymptotic approach is its ability to reduce this complex phenomenon to an analytic expression which can be used to understand the physics of the ignition criterion.

Ignition Behavior

The bifurcation factor, Δ_B, determines how the solution will behave as the concentration of the hydrogen radical, ϵ, increases. When Δ_B is negative, increases in ϵ result in a decrease in Δ. Therefore, there is a turning point in the steady state solution and the system will ignite abruptly. When Δ_B is positive, increases in ϵ result in an increase in Δ. In this case, the system will monotonically transition to an ignited state. The bifurcation factor can be solved for from Eq. (17) or determined using the following compatibility condition which results from integration of the self-adjoint form of that

equation:

$$\Delta_B = \int_{-\infty}^{\infty} \Delta_I y_{H,1}^2 \left[2k_{1,f} \left(-Y_{O_2,f} \frac{T_{a,1}}{T_f^2} \phi + y_{O_2,1} + Y_{O_2,f} \frac{k_{12,f} y_{HO_2,1}}{k_{2,f} Y_{H_2,f}} \right) \right.$$
$$\left. - k_{9,f} y_{O_2,1} - k_{11,f} \left(1 - \frac{k_{10,f}}{k_{11,f}} \right) y_{HO_2,1} \right] e^{x^2/2} dx \qquad (24)$$
$$/ \int_{-\infty}^{\infty} y_{H,1}^2 \left[2k_{1,f} - k_{9,f} \right] e^{x^2/2} dx.$$

Expanding for small Lewis number further simplifies this expression. Due to the small diffusivity of O_2 and HO_2 relative to H, not only is the oxygen concentration exponentially small in the low temperature stream, but the HO_2 radical concentration is also exponentially small. Therefore, the contribution of the integral from $-\infty$ to $-x$ of $O(\sqrt{Le_H})$ can be neglected. Additionally, as a first approximation the $O(\sqrt{Le_H})$ contribution from the zone around the stagnation plane can also be neglected. Our final simplification is to normalize $y_{HO_2,1}$, $y_{O_2,1}$, and ϕ_1 by the coefficient of $y_{H,1}$ in equations (13)-(15) respectively. This results in the following simplified expression for the bifurcation factor:

$$\Delta_B = \int_0^{\infty} \Delta_I y_{H,1}^2 \left\{ -2 \frac{T_{a,1}}{T_\infty^2} (q_1^* + q_9 k_{9,\infty}) \overline{\phi} + (1 + k_{9,\infty})(2 - k_{9,\infty}) \overline{y}_{O_2,1} \right.$$
$$\left. - \left[k_{11,\infty} \left(1 - \frac{k_{10,\infty}}{k_{11,\infty}} \right) - \frac{k_{12,\infty}}{k_{2,\infty} Y_{H_2,f}} \right] k_{9,\infty} \overline{y}_{HO_2,1} \right\} e^{x^2/2} dx$$
$$/ \int_{-\infty}^{\infty} y_{H,1}^2 \left[2k_{1,f} - k_{9,f} \right] e^{x^2/2} dx. \qquad (25)$$

Insight into the controlling mechanism of the ignition behavior can be gained by examining the terms of this equation. The coefficient of $\overline{\phi}$ in this equation represents the effect of heat release on the bifurcation factor. Because of the large activation energy of the branching reaction, heat addition to the system causes the rate of reaction 1 to exponentially increase while the termination reaction remains relatively insensitive to heat addition. Therefore, the net branching rate increases causing the solution to exhibit a turning point. The magnitude of this effect is proportional to the heat release from the branching and termination steps and to the activation temperature. Its

dependence on the activation energy reflects the nature of the Arrhenius term. Large activation energy relative to the flow temperature indicates that only a small fraction of the possible branching collisions have enough energy to react. In this case, the branching rate will be very sensitive to heat release. At higher system temperatures a greater percentage of the collisions react and the system is less sensitive to heat release.

The second term in the compatibility condition is due to the effect of oxygen depletion on the ignition process. Depletion of oxygen causes a decrease in the net branching rate. The magnitude of this effect is proportional to the amount of oxygen depletion, $(k_1 + k_9)$ as found from Eq. (14), times the net branching rate, $(2k_1 - k_9)$. The sign of this bifurcation parameter is positive, meaning that oxygen depletion will reduce the net branching rate and lead to a monotonic ignition phenomenon.

The remaining terms in the bifurcation factor are due to the effect of HO_2 chemistry. These terms are all proportional to k_9 because this reaction determines the production rate of HO_2. Because reaction 9 is a three body reaction, its production rate of HO_2 is slow at low pressures. Therefore, reactions involving HO_2 are unimportant at low pressures. At higher pressures, however, production of HO_2 is not negligible, and HO_2 chemistry can have several significant effects. Reaction 11, $H + HO_2 \rightarrow 2OH$, is an additional branching step for the hydrogen radical, while reaction 10, $H + HO_2 \rightarrow H_2 + O_2$, is a termination step. The ratio of the rates of these reactions is nearly independent of temperature with k_{10}/k_{11} being approximately 1/6. Lumping these two reactions together, the net effect is the production of an additional 5/6 of a hydrogen radical for every reaction between H and HO_2. Thus as HO_2 is produced, there is an additional source of branching for the hydrogen radical. This accelerates the ignition process and leads to a turning point in the steady state solution.

The final term is due to the effect of reaction 12 on the steady state approximation for the oxygen radical. Reaction 12 competes with reaction

2 for oxygen radicals:

$$\begin{aligned} R2 \quad & O + H_2 \rightarrow OH + H, \\ R12 \quad & O + HO_2 \rightarrow OH + O_2. \end{aligned} \tag{26}$$

While reaction 2 is a branching step, reaction 12 is only a propagation step. At low HO_2 concentrations most of the radicals are consumed by reaction 2. However at larger HO_2 concentrations more O radicals are consumed by reaction 12, and the net branching rate decreases. The bifurcation parameter is a ratio of the rates of these two pathways. The sign of this term indicates that as HO_2 accumulates there will be a reduction in the net branching rate. The dependence of reaction 2 on the H_2 concentration is also apparent. Increasing the hydrogen concentration increases the rate of reaction 2 and thus diminishes the importance of reaction 12 in determining the bifurcation factor.

At different pressures, temperatures, and fuel concentrations any one of these nonlinear effects can control the ignition process. In figure 4, the bifurcation parameters associated with heat release, oxygen depletion, and reactions 10 and 11 calculated along the ignition curve of $a = 1000s^{-1}$ are plotted as a function of temperature. The effect of reaction 12 will be examined subsequently because of its dependence on the fuel concentration. In the second limit, the termination rate k_9 is $O(1)$, and the ignition mechanism is dominated by the effect of the reaction $H + HO_2 \rightarrow 2OH$. In the first ignition limit, k_9 becomes $\ll 1$, and the effect of heat release becomes the dominant effect. At very low pressures, the ignition temperature increases, and, as discussed, the effect of heat release diminishes. Oxygen depletion then competes with heat release in determining the ignition behavior. Figure 4 demonstrates the various responses that can be exhibited by the hydrogen-oxygen system at different ignition pressures and temperatures.

The bifurcation parameter associated with reaction 12 and the parameter due to reactions 10 and 11 are plotted along the ignition curve of

$a = 1000s^{-1}$ for various fuel concentrations in figure 5. This figure shows that these two bifurcation parameters exhibit similar temperature dependence. In addition, for H_2 concentrations in the reaction zone for which the steady state assumption still holds, i.e. $Y_{H_2,f}k_2 \gg 1$, the effect of reaction 12 is always dominated by reaction 11. Only for small fuel concentrations will reaction 12 have a significant effect.

Figure 6 shows the bifurcation factor calculated from the compatibility condition along the ignition curve of $a = 1000s^{-1}$ for an incoming stream of pure hydrogen. Only the bifurcation factor calculated along the first limit is shown. In the second limit, the bifurcation factor is negative with a magnitude $\gg 1$ due to the strong effect of reaction 11. This figure shows that around 2000K the bifurcation factor crosses zero. This is in agreement with figure 4 which shows that at this temperature the effects of heat release and oxygen depletion are of the same order. Above this temperature, the bifurcation factor becomes positive, and the system no longer ignites abruptly.

Finally, the ignition temperatures and pressures are plotted in figure 7 with curves delineating the transition between ignition through HO_2 branching, ignition through heat release, and the monotonic transition caused by oxygen depletion in the reaction zone. These curves were calculated by equating the relevant bifurcation parameters. In each of the regimes, the ignition criterion is still determined by a balance between branching, termination, and convective-diffusive loss of the hydrogen radical, but the mechanism by which the system ignites is different. In regime I, $H + HO_2 \rightarrow 2OH$ accelerates the net branching rate and causes the system to ignite abruptly. In regime II, heat release accelerates the branching rate by its effect on the Arrhenius term of reaction 1, and again the system abruptly ignites. Regime III is the monotonic transition region. As the Damköhler number is increased, diffusion of oxygen limits the system, and the system will monotonically transition to an ignited state. In these ignition processes, once the

system becomes unstable and begins to transition to an ignited state, we note that other effects become important. As the system ignites in regime I, eventually heat release will also contribute to the transition to a diffusion flame. It is only the mechanism by which ignition is initiated which is considered here.

Conclusions

Ignition of a hydrogen-oxygen counterflow system for temperatures above the crossover temperature was studied asymptotically using eight elementary steps to describe the high temperature ignition reaction mechanism. For $O(1)$ fuel concentrations, chemical steady state of O and OH were shown to be justifiable approximations, and a simplified reduced mechanism was derived. Using this reduced mechanism, we were able to verify the fact that hydrogen-oxygen ignition is determined by a balance between branching, termination, and transport of the hydrogen radical. In addition, an algebraic ignition criterion was found which predicted ignition limits analogous to the first and second limit of the homogeneous hydrogen-oxygen system. This criterion clarified the physics underlying the behavior of these limits, and captured the dependence of the ignition limits on all system parameters.

Performing a bifurcation analysis similar to that of Sánchez *et al.* (1994), the ignition behavior of the hydrogen-oxygen system was also resolved. We found that for temperatures above the crossover temperature, abrupt ignition can occur either through interactions between H and HO_2 via the reaction $H + HO_2 \rightarrow 2OH$, or through the effect of heat release on the branching rate. At temperatures much greater than the crossover temperature, oxygen depletion in the ignition zone can cause the system to exhibit a monotonic transition to the ignited state.

Acknowledgment

Dr. T. G. Kreutz of Princeton University is gratefully acknowledged for his advice, insight, and patience in discussions of this problem. This work was supported in part by the Army Research Office and the Air Force Office of Scientific Research under the technical monitoring of Drs. D. M. Mann and J. M. Tishkoff respectively.

References

Abromowitz, M. and Stegun, I. A. 1965 *Handbook of Mathematical Functions*, pp. 686-689. New York: Dover.

Balakrishnan, G., Smooke, M. D. and Williams, F. A. 1995 A Numerical Investigation of Extinction and Ignition Limits in Laminar Nonpremixed Counterflowing Hydrogen-Air Streams for Both Elementary and Reduced Chemistry. *Combust. Flame*, in press.

Baulch, D. L., Drysdale, D. D., Horne, D. G. and Llyod, A. C. 1972 *Evaluated Kinetic Data for High Temperature Reaction, Vol. 1: Homogeneous Gas Phase Reactions of the H-O System.* London: Butterworths.

Darabiha, N. and Candel, S. 1992 The Influence of the Temperature on Extinction and Ignition Limits of Strained Hydrogen-Air Diffusion Flames. *Combust. Sci. Tech.* 86, 67-85.

Kreutz, T. G. and Law, C. K. 1993 Ignition in Nonpremixed Counterflowing Hydrogen versus Heated Air: I. Computational Study with Detailed and Simplified Chemistry. Paper No. 92 presented at the 1993 Joint Technical Meeting of the Central and Eastern States Sections of the Combustion Institute, New Orleans, LA, March 15-17.

Kreutz, T. G., Fotache, C., and Law, C. K. 1994 Computational and Experimental Studies of Ignition in Nonpremixed Counterflowing Hydrogen versus Heated Air. Paper No. 77 presented at the Spring 1994 Technical Meeting of the Central States Section of the Combustion Institute, University of Wisconsin, Madison, WI, June 5-7.

Kreutz, T. G., Nishioka, M., and Law, C. K. 1994 The Role of Kinetic versus Thermal Feedback in Nonpremixed Ignition of Hydrogen versus Heated Air. *Combust. Flame*, 99, 758-766.

Kreutz, T. G. and Law, C. K. 1995 Ignition in Nonpremixed Counterflowing

Hydrogen versus Heated Air: Computational Study with Detailed Chemistry. *Combust. Flame*, in press.

Lee, S. R. and Law, C. K. 1994 Asymptotic Analysis of Ignition in Nonpremixed Counterflowing Hydrogen versus Heated Air. *Combust. Sci. Tech.*, **97**, 377-389.

Liñán, A. 1974 The Asymptotic Structure of Counterflow Diffusion Flames for Large Activation Energies. *Acta Astronautica*, **1**, 1007-1039.

Maas, U. and Warnatz, J. 1988 Ignition Processes in Hydrogen-Oxygen Mixtures. *Combust. Flame*, **74**, 53-69.

Sánchez, A. L., Liñán, A., and Williams, F. A. 1994 A Bifurcation Analysis of High-Temperature Ignition of H_2-O_2 Diffusion Flames. *Twenty-Fifth Symposium (International) on Combustion*, pp. 1529-1537. Pittsburgh: The Combustion Institute

Treviño, C. 1991 Ignition Phenomena in H_2-O_2 Mixtures, in *Dynamics of Deflagrations and Reactive Systems: Flames*, (ed. A. L. Kuhl, J. C. Leyer, A. A. Borisov & W. A. Sirignano), Progress in Astronautics and Aeronautics, AIAA, **131**, pp. 19-43.

Vlachos, D. G., Schmidt, L. D., and Aris, R. 1993 Ignition and Extinction of Flames Near Surfaces: Combustion of H_2 in Air. *Combust. Flame*, **95**, 313-335.

Warnatz, J. 1984 Rate Coefficients in the C/H/O System, in *Combustion Chemistry*, (ed. W. C. Gardiner, Jr.), pp. 197-360. New York: Springer-Verlag.

Yetter, R. A., Dryer, F. L., and Rabitz, H. 1991 A Comprehensive Reaction Mechanism for Carbon Monoxide/Hydrogen/Oxygen Kinetics. *Combust. Sci. Tech.*, **79**, 97-128.

Appendix A

When using the activation energy as a large expansion parameter, the physical domain can be divided into three zones. In the high temperature stream, there is a zone in which $T = T_\infty$ and $Y_{O_2} = 1$. This is followed by a thin zone in which the branching rate exponentially decays and then a convective-diffusive-termination zone. In the upstream zone, the solution for the hydrogen radical is the same as in the small Lewis number case, $e^{-Le_H x^2/4} U(1/2 - \Delta, x\sqrt{Le_H})$, where x is now made nondimensional by the thermal length, $\sqrt{\lambda/\rho c_p a}$, and U is the parabolic cylinder function (Abromowitz and Stegun, 1965). In the inner zone, the solution satisfies the equation:

$$\left(\frac{1}{Le_H} - 1\right)\xi\frac{dY_H}{d\xi} + \frac{1}{Le_H}\frac{d^2Y_H}{d\xi^2} = -\Delta Y_H\left[2e^{-\xi} - k_9\right], \qquad \text{(A1)}$$

where $\xi = e^{-(x-x_r)x_r}$ and x_r is the large expansion parameter which is determined by the location of the decay zone. The matching zone for the high temperature stream and the inner solution is $x_r^{-1} \ll (x - x_r) \ll x_r$. To match these solutions, an expansion for $e^{-Le_H x^2/4} U(1/2 - \Delta, x\sqrt{Le_H})$ is needed around the point x_r. Normally, x_r is a large number and a large-x expansion can be used, but because the coupling $x_r\sqrt{Le_H}$ is actually less than one, this method would be inappropriate. Furthermore, once the matching condition was derived, equation (A1) would still need to be solved numerically to determine the ignition Damköhler number.

The small Lewis number method (Sánchez *et al.*, 1994) allows us to avoid these difficulties and obtain an analytic expression for the ignition Damköhler number. It is also a more appropriate expansion parameter because the large activation energy expansion parameter x_r is only slightly larger than one, whereas the Lewis number is $O(10^{-1})$.

Appendix B

The solution in the high temperature chemical steady state region is:

$$c_1 e^{-x^2/4} U(1/2-\Delta, x) + c_2 e^{-x^2/4} V(1/2-\Delta, x), \tag{B1}$$

where U and V are the parabolic cylinder functions (Abromowitz and Stegun, 1965). Assuming that this solution is valid through the region where the steady state approximations degenerate, we can find a relation between c_1 and c_2 by enforcing the condition that $Y_H = 0$ at the high temperature boundary. Using the large-x expansions for these functions the following equation is arrived at:

$$c_1 e^{-x_b^2/2} x_b^{\Delta-1} + c_2 x_b^{-\Delta} = 0, \quad \text{or} \quad c_2/c_1 = e^{-x_b^2/2} x_b^{2\Delta-1}, \tag{B2}$$

where x_b is the boundary location. In the limit of $x_b \to \infty$, we see that c_2 is negligible and the solution in the high temperature stream is $c_1 e^{-x^2/4} U(1/2-\Delta, x)$.

When reaction is assumed frozen in the region where the chemical steady state approximations degenerate, we need to perform matching between the frozen region and the chemical steady state region. In the frozen region we have the solution $d_1 + d_2 \mathrm{erfc}(x/\sqrt{2})$, and in the chemical steady state region the solution is again as in equation (B1). Enforcing the high temperature boundary condition to the frozen solution in the limit of the boundary location going to infinity results in the solution $d_2 \mathrm{erfc}(x/\sqrt{2})$ in the frozen zone. If we match slopes and values between the frozen solution and the steady state zone solution at a location where $x \gg 1$ but the steady state approximations are still valid, we get:

$$d_2 \frac{e^{-x_f^2/2}}{\sqrt{2\pi} x_f} = c_1 e^{-x_f^2/2} + c_2 x_f^{-\Delta}, \tag{B3}$$

$$-d_2 \frac{e^{-x_f^2/2}}{\sqrt{2\pi}} = c_1 e^{-x_f^2/2} \left(x_f^{-\Delta} - (\Delta - 1) x_f^{\Delta-2} \right) - c_2 \Delta x_f^{-\Delta-1}. \tag{B4}$$

Solving for the ratio c_2/c_1 gives:

$$\frac{c_2}{c_1} = \frac{e^{-x_f^2/2}}{\sqrt{2\pi}}(\Delta - 1)x_f^{2\Delta-3}, \tag{B5}$$

where x_f is the matching location. This ratio is again exponentially small for $x_f \gg 1$. The solution in the steady state region is the same for both cases, which shows that the non-steady state region has little importance in determining the ignition criterion. However, if the incoming fuel concentration becomes $\ll 1$, then the steady state approximations will break down for x of $O(1)$ and there will indeed be an effect on the ignition criterion due to the breakdown in the steady state approximations.

Figure Captions

Figure 1 Comparison of numerical solutions for maximum Y_H with and without initiation reaction.

Figure 2 Schematic of the frozen temperature, oxygen, and hydrogen profiles in each asymptotic zone.

Figure 3 Pressure and temperature ignition limits for various strain rates.

Figure 4 Bifurcation parameters of reactions 10 and 11, heat release, and oxygen depletion along the first and second ignition limits of $a = 1000s^{-1}$.

Figure 5 Bifurcation parameters of reactions 10 and 11, and reaction 12 along the first and second ignition limits of $a = 1000s^{-1}$ for various fuel concentrations.

Figure 6 The bifurcation factor, Δ_B, along the first ignition limit of $a = 1000s^{-1}$.

Figure 7 High temperature ignition regimes of the hydrogen-oxygen system.

Table 1 Starting reaction mechanism for the hydrogen-oxygen system. Rate constants are in the form $k = AT^n \exp(-E_a/R^\circ T)$. Units are moles, cm^3, seconds, Kelvin and kcal/mole.

no.	reaction	A	n	E_a
R1	$H + O_2 \rightarrow O + OH$	1.92E+14	0.00	16.44
R2	$O + H_2 \rightarrow H + OH$	5.08E+04	2.67	6.29
R3	$OH + H_2 \rightarrow H + H_2O$	2.16E+08	1.51	3.43
R9	$H + O_2 + M \rightarrow HO_2 + M$	6.17E+19	−1.42	0.00
R10	$HO_2 + H \rightarrow H_2 + O_2$	6.63E+13	0.00	2.13
R10b	$H_2 + O_2 \rightarrow HO_2 + H$	1.93E+14	0.00	59.61
R11	$HO_2 + H \rightarrow OH + OH$	1.69E+14	0.00	0.87
R12	$HO_2 + O \rightarrow OH + O_2$	1.81E+13	0.00	-0.40

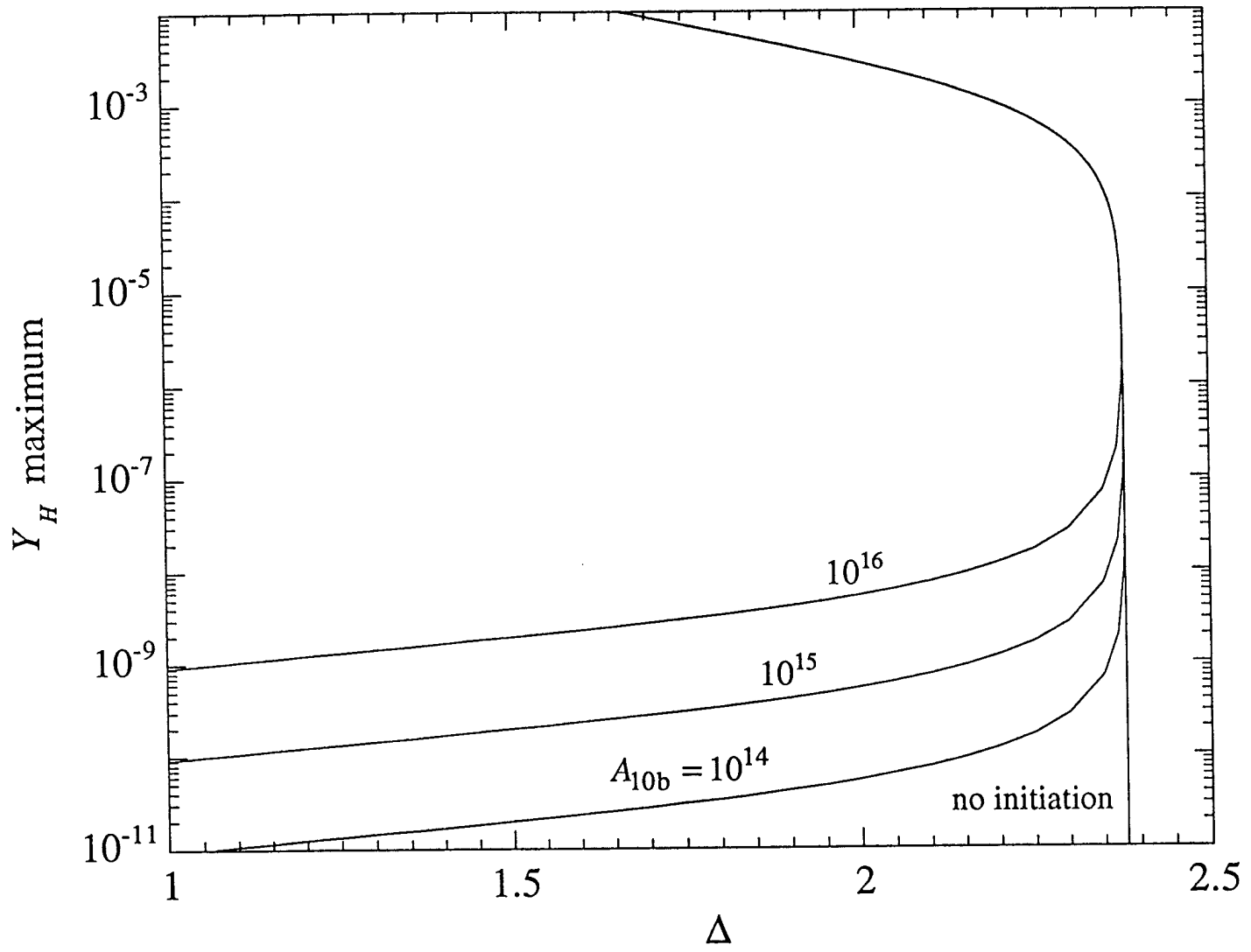
10^{-3}
10^{-5}
10^{-7}
10^{-9}
10^{-11}
Y_H maximum
10^{16}
10^{15}
$A_{10b} = 10^{14}$
no initiation
1
1.5
2
2.5
Δ

figure 1

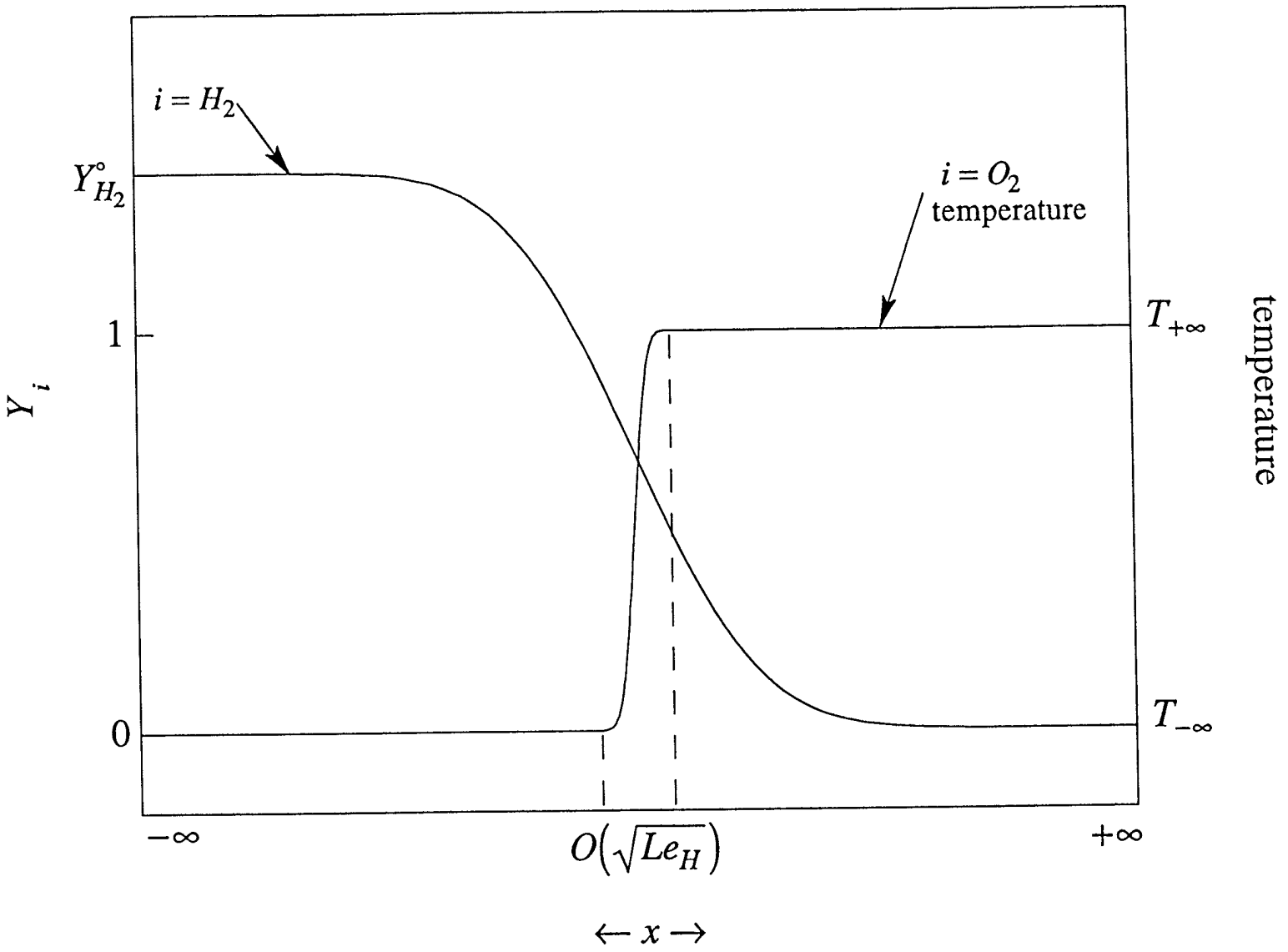
$i = H_2$
$Y^{\circ}_{H_2}$
$i = O_2$
temperature
1
Y_i
$T_{+\infty}$
temperature
$T_{-\infty}$
0
$-\infty$
$O\left(\sqrt{Le_H}\right)$
$+\infty$
$\leftarrow x \rightarrow$

figure 2

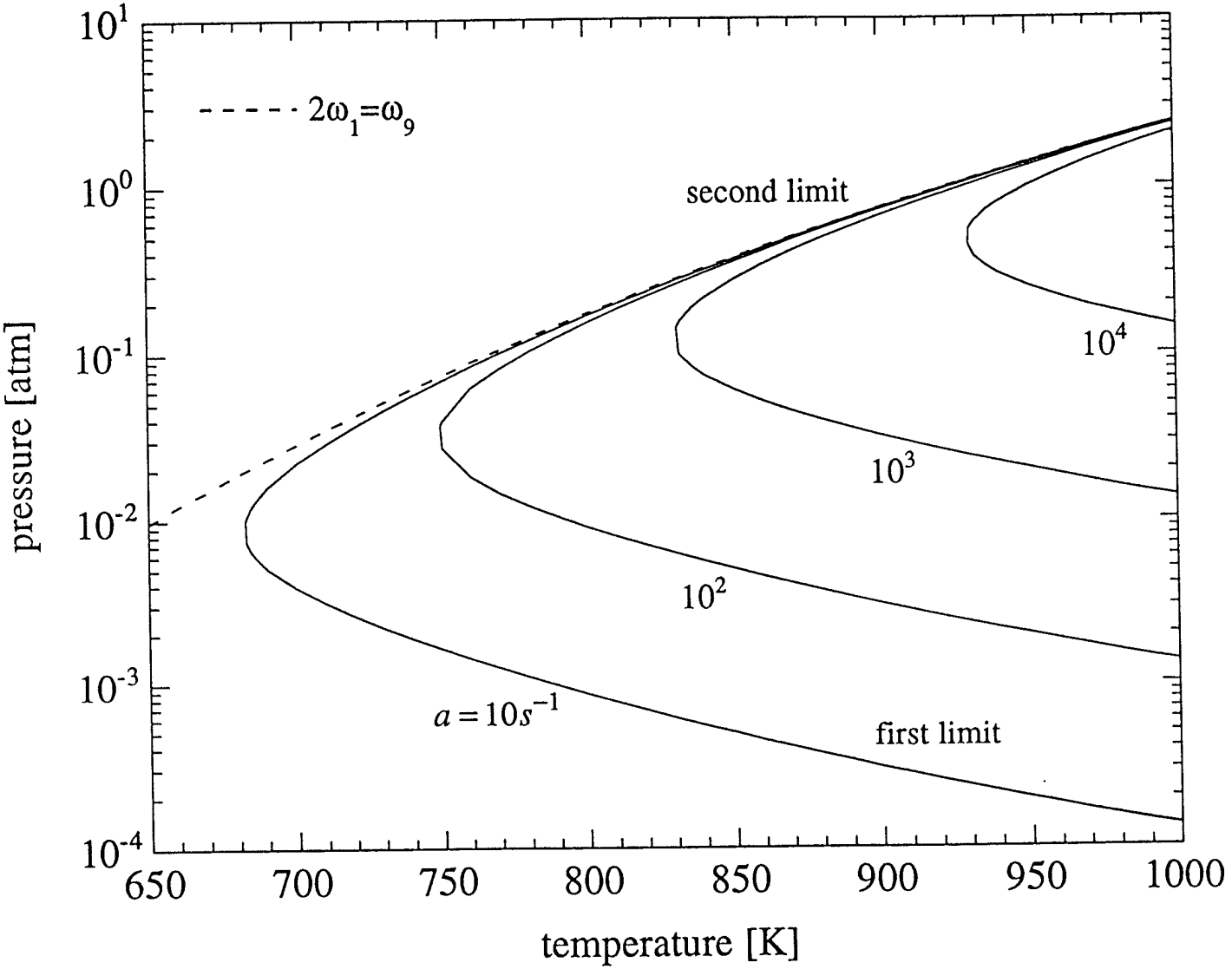
10^1
10^0
10^{-1}
10^{-2}
10^{-3}
10^{-4}
pressure [atm]
$2\omega_1=\omega_9$
second limit
10^4
10^3
10^2
$a=10s^{-1}$
first limit
650
700
750
800
850
900
950
1000
temperature [K]

figure 3

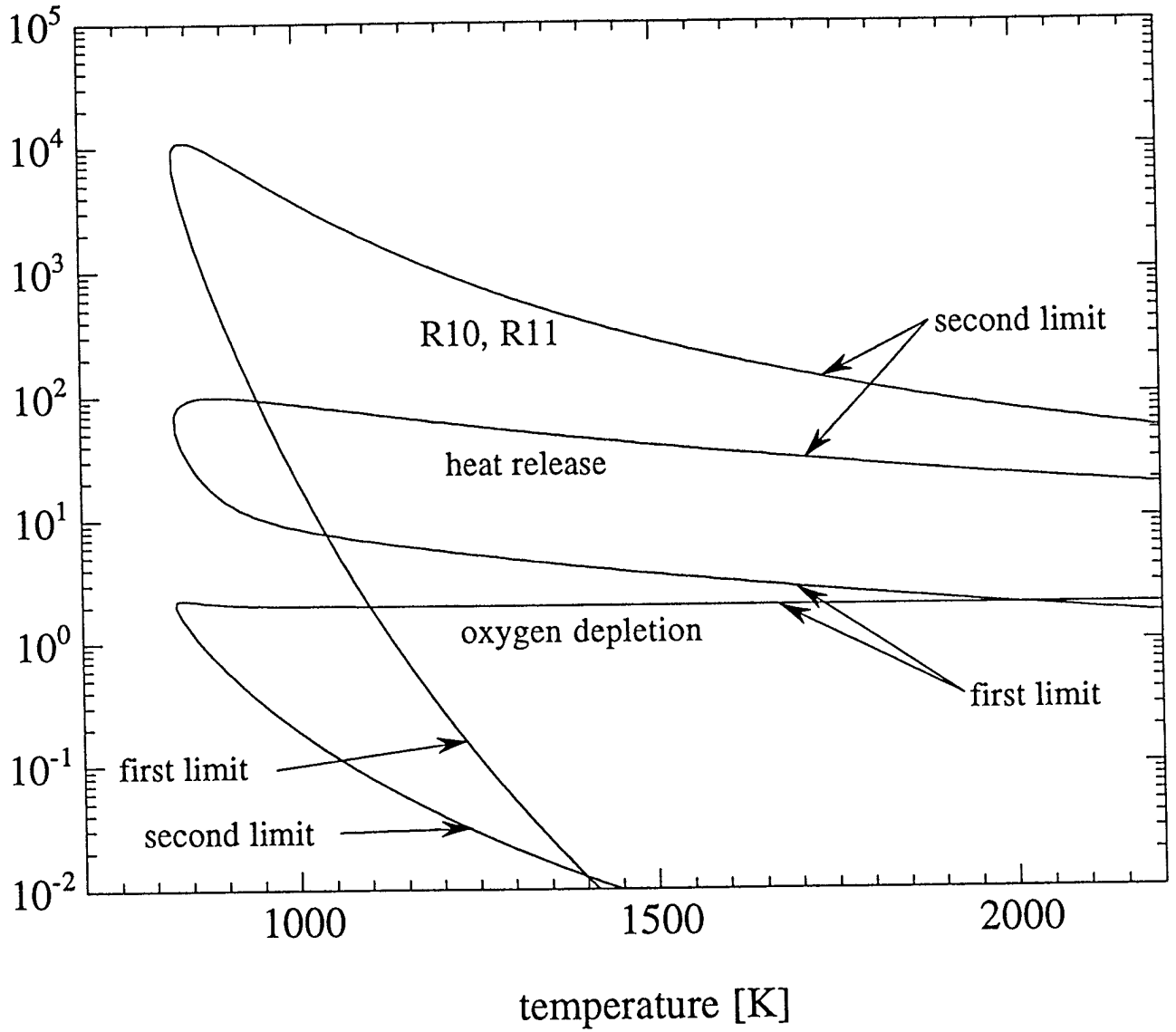
10^5
10^4
10^3
10^2
10^1
10^0
10^{-1}
10^{-2}
R10, R11
second limit
heat release
oxygen depletion
first limit
first limit
second limit
1000
1500
2000
temperature [K]

figure 4

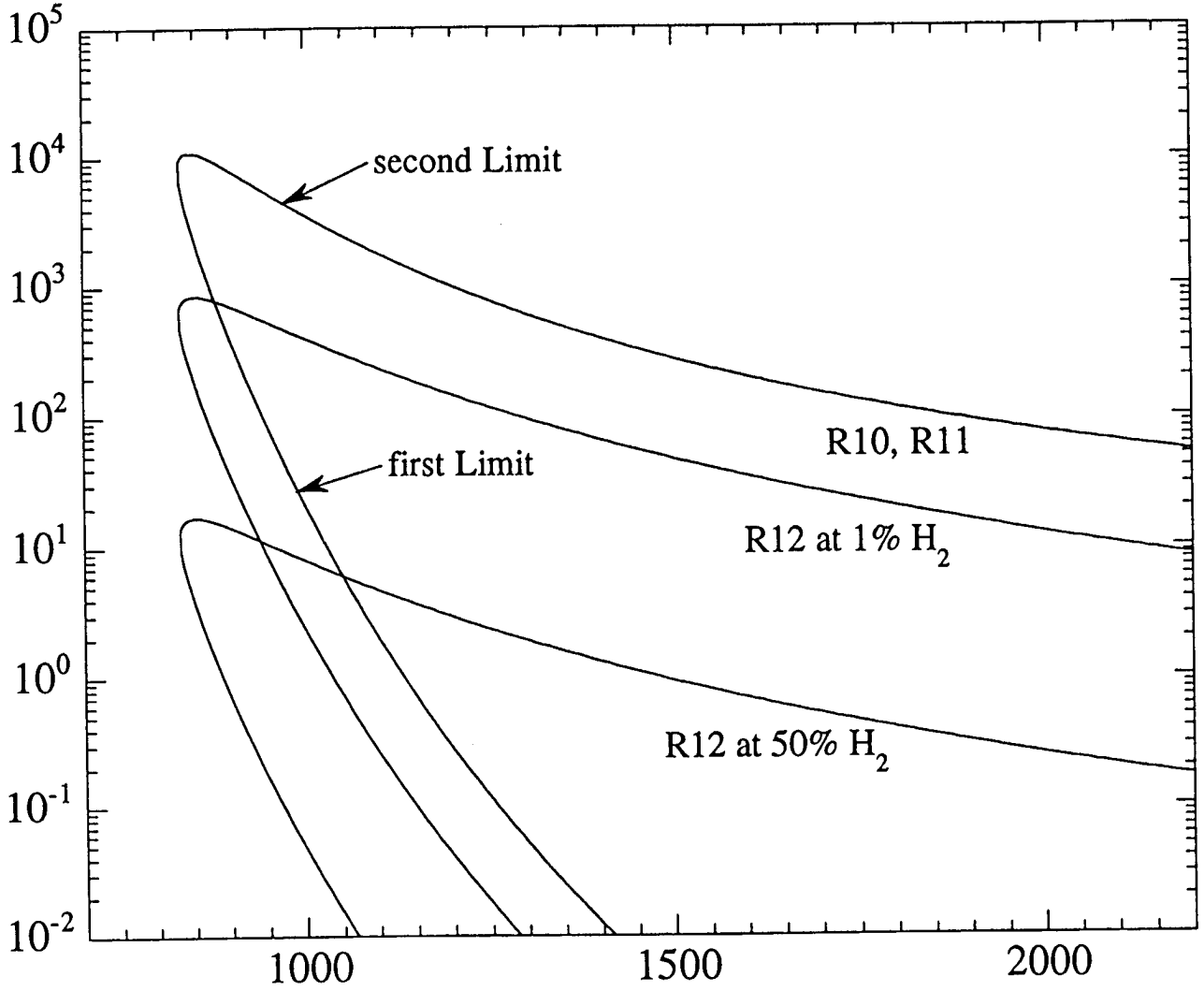
10^5
10^4
10^3
10^2
10^1
10^0
10^{-1}
10^{-2}
second Limit
first Limit
R10, R11
R12 at 1% H_2
R12 at 50% H_2
1000
1500
2000
temperature [K]

figure 5

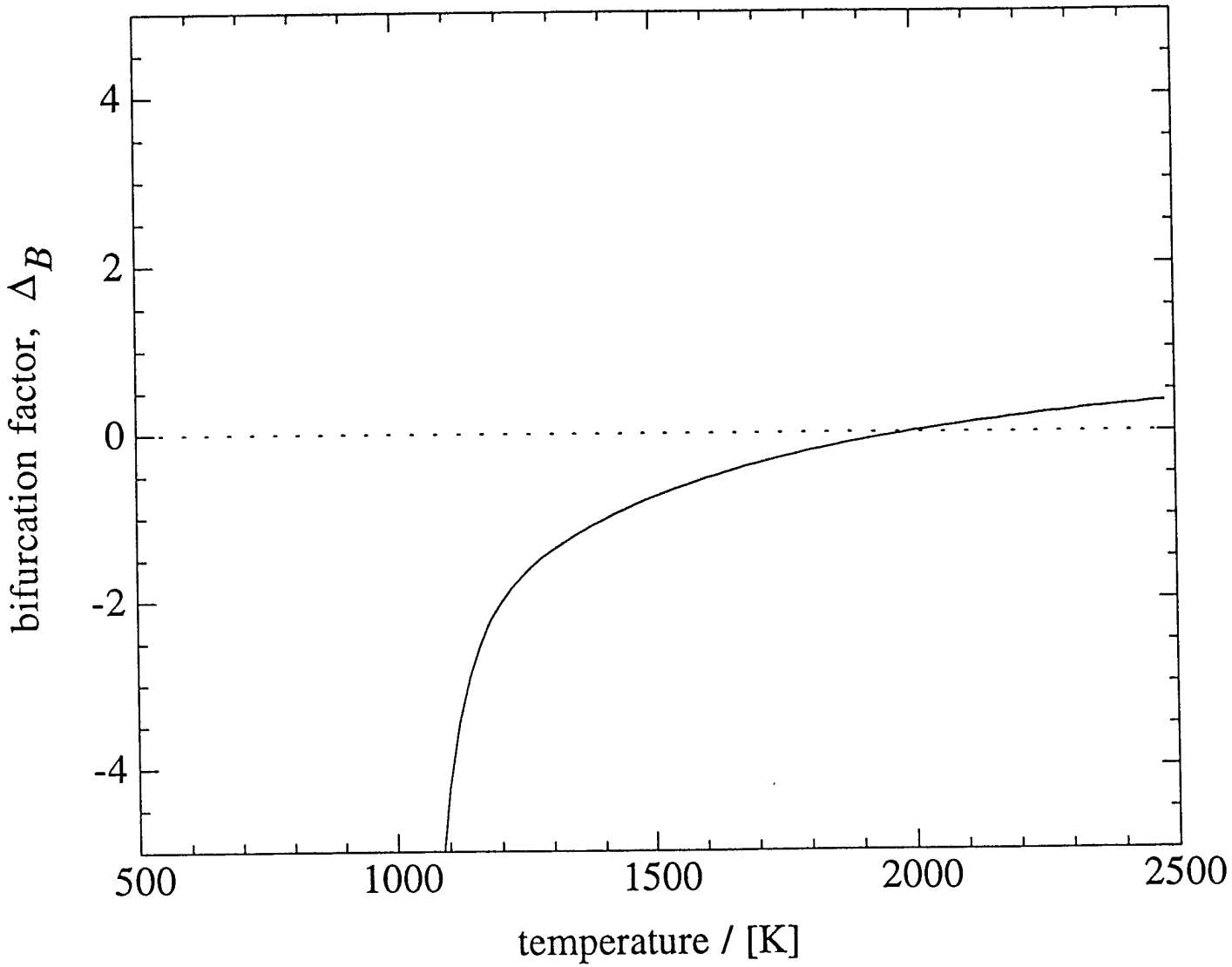
bifurcation factor, Δ_B
4
2
0
-2
-4
500
1000
1500
2000
2500
temperature / [K]

figure 6

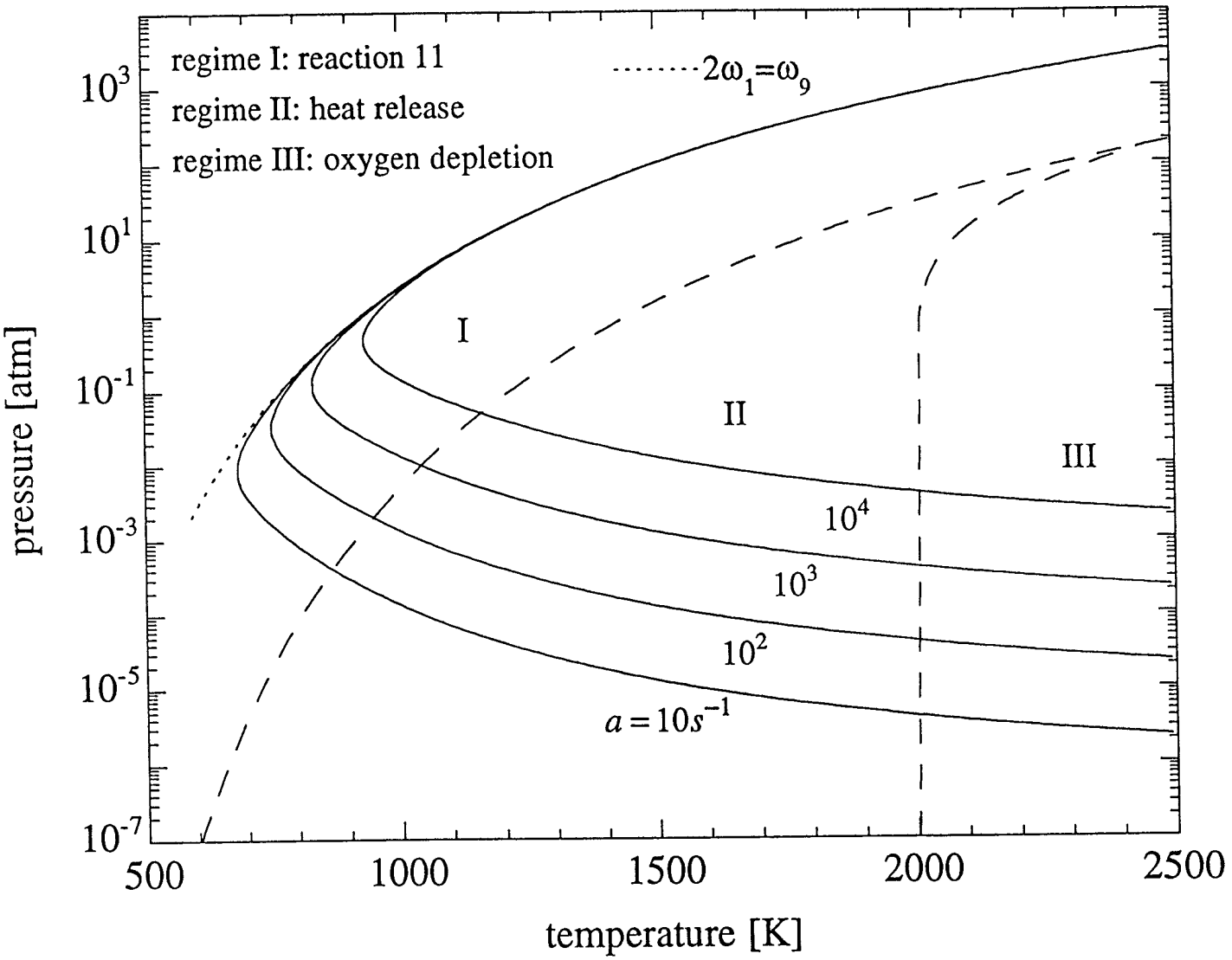
regime I: reaction 11
regime II: heat release
regime III: oxygen depletion
$2\omega_1=\omega_9$
I
II
III
10^4
10^3
10^2
$a=10s^{-1}$
pressure [atm]
10^3
10^1
10^{-1}
10^{-3}
10^{-5}
10^{-7}
500
1000
1500
2000
2500
temperature [K]

figure 7